RICE UNIVERSITY

Zinc Exchanged Carbonate Minerals: Application for *in situ* Treatment of Arsenic Contaminated Groundwater

by

Jonathan Aaron Pennington

A THESIS SUBMITTED
IN PARTIAL FULFILLMENT OF THE
REQUIREMENTS FOR THE DEGREE

Master of Science

APPROVED, THESIS COMMITTEE:

Mason Tomson, Professor, Chair
Civil and Environmental Engineering

C. Herb Ward, Foyt Family Chair,
Civil and Environmental Engineering

Philip Bedient, Herman Brown Professor,
Civil and Environmental Engineering

HOUSTON, TEXAS
May 2012

ABSTRACT

Zinc Exchanged Carbonate Minerals: Application for *in situ* Treatment of Arsenic Contaminated Groundwater

By

Jonathan Aaron Pennington

While over 140 million people worldwide are at risk of drinking arsenic contaminated groundwater above the WHO guideline of 10 μg/L, the need for an efficient treatment scheme in actual groundwater conditions is growing. This study examines the use of zinc carbonate minerals for *in situ* removal of As(V) from contaminated groundwater. Batch adsorption isotherms compare the adsorption of As(V) to reagent grade $ZnCO_3$ and freshly precipitated $ZnCO_3$ minerals on calcite particles in buffered electrolyte solution and real groundwater. Column studies examine the exchange of calcite particles for zinc-carbonate minerals through injection of a zinc chloride solution and the subsequent removal of As(V). While arsenic adsorption in batch studies is greatly reduced in actual groundwater relative to synthetic solution, As(V) mobility is significantly impeded in column studies with R greater than 12,000 for both synthetic and actual groundwater. Plausible explanations for arsenic removal mechanisms are discussed.

ACKNOWLEDGEMENTS

This work could never have been accomplished without the fervent support of so many people to whom I am gratefully indebted. First, I would like to thank my advisor, Dr. Mason Tomson, for the countless hours of guidance and advice he has contributed to my growth over the past two years. I am also appreciative towards committee members Dr. Herb Ward and Dr. Phil Bedient for their assistance which contributed to my understanding and implementation of this work.

A special thanks to Dr. Amy Kan for all of the time and advice she contributed to helping bring this work to fruition. I would also like to thank all the fellow members from the Tomson lab over the past two years including Chunfang Fan, Jie Yu, Haiping Lu, Hualin Li, Essmaiil Djamali, Chao Yan, Wei Shi, Wei Wang, Lu Wang, Nan Zhang, Zhang Zhang, Ping Zhang, Hamad Alsaiari, Sarah Work, and Jesse Farrell for the helpful discussion and encouragement during the ups and downs of research.

I also owe a large thanks to Debbie, Jerry, Josh, and Denise and the rest of the family for their loving support through this experience and to all my close friends at Faithbridge for their encouragement over the past year. Above all else, I praise God for sustaining me with grace, truth, and love throughout this time.

This research was supported by the National Science Foundation through the Graduate Research Fellowship Program.

TABLE OF CONTENTS

List of Figures

List of Tables

1. Introduction

Arsenic contamination of groundwater is a major global issue with over 140 million people in more than 70 countries at risk of drinking unsafe levels of arsenic (Ravenscroft, 2007). Both acute and chronic exposure to arsenic have been documented to cause a variety of health impairments including skin lesions, renal failure, cardiovascular disease, and cancer. While conventional treatment methods such as coagulation/flocculation, ion-exchange, adsorptive media, and reverse osmosis are effective at removing arsenic from source water to safe levels, they are subject to high operation and maintenance needs, decreased treatment efficiency based upon water quality parameters, and generally more cost-effective at the community wide level. Therefore, more focus has recently been placed on the use of innovative *in situ* treatment technologies.

Some unconventional treatment schemes include the use of phytoremediation or zero-valent iron for arsenic adsorption onto corrosion byproducts. One of the most effective *in situ* treatment designs involves the use of a permeable reactive barrier, in which groundwater is passively treated by flowing through a zone of emplaced reactive media. However, traditional reactive barriers require high labor and installation costs for initial emplacement, are limited on depth of treatment zone, and must physically replace media once exhausted. A more sustainable and effective media barrier should take advantage of solution chemistry in order to inject a reactive solution into the aquifer matrix and precipitate the reactive media.

The aim of this work is to investigate the use of a zinc-exchanged calcite media for arsenic adsorption. Specifically, the adsorption of As(V) onto $ZnCO_3$ will be

examined in batch and column experiments under both synthetic water and actual Rice groundwater solutions.

Organization of Thesis

Section 2 of this thesis covers background information in this area of study. Briefly, the literature review covers arsenic occurrence and toxicity, conventional arsenic treatment methods, *in situ* arsenic treatment methods, the significance of carbonate aquifers, basic theory on mineral dissolution and precipitation, zinc occurrence and toxicity, and background on column adsorption and transport modeling studies. The next section of this thesis details the methods and materials used in this work, whereas section 4 provides the results of these experiments and discussion.

2. Background and Review of Current Literature

Arsenic Occurrence & Toxicity

Arsenic is a metalloid naturally present in the Earth's crust as the 20th most prevalent element with an average concentration of 2-3 mg As / kg in continental crust (Cullen, 1989; Tanaka, 1988). It is a major component of over 200 known minerals including arsenides, sulphides, oxides, arsenates, arsenites, and elemental As. Though most As-bearing minerals are quite rare in the environment, the most abundant As mineral is arsenopyrite, FeAsS (Smedley and Kinniburgh, 2002).

Arsenic concentrations in fresh water are highly variable depending on the source of arsenic and local geochemical environment. Two major sources of arsenic into the environment include 1) release from natural processes and 2) anthropogenic activities. Natural processes that remobilize As include volcanic activity, mineral dissolution, plant expungement, and particulate transport by wind. The primary mechanisms affecting groundwater As contamination include geothermal groundwater inputs, mineral dissolution, and changes in the redox potential leading to As desorption and/or dissolution (Smedley and Kinniburgh, 2002). Anthropogenic activity can also lead to reintroduction of previously immobilized As into the atmosphere and hydrosphere, such as mining, metal smelting, and fossil fuel combustion. Multiple industries also employ As in the manufacturing of products such as wood preservatives, pesticides, alloys, glass, leather preservatives, pigments, anti-fouling paints, and poison baits, which can lead to soil and water contamination through widespread use and improper disposal (WHO, 2010).

While Arsenic is observed in nature in the oxidation states -3, 0, +3, and +5, it most commonly occurs in natural waters as the inorganic oxyanion of trivalent arsenite (III) or pentavalent arsenate (V). The speciation of arsenic in waters is most dependent upon pH and redox potential, Eh, as can be seen in Figure 1.

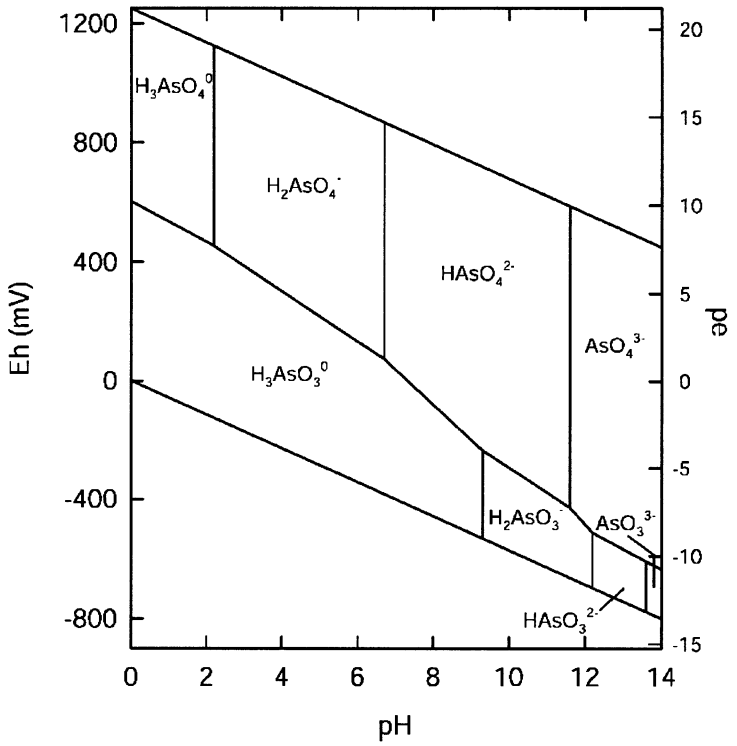

Figure 1: Pourbaix diagram for the As-O_2-H_2O system at 25 C and 1 bar (Brookins, 1988)

Under acidic oxidizing conditions (pH < 6.9), $H_2AsO_4^-$ is the predominant species while at pH > 6.9 $HAsO_4^{2-}$ predominates. Likewise under reducing conditions, H_3AsO_3 is the predominant species at all typical pH values of natural waters, and $H_2AsO_3^-$ predominates at pH > 9.2. It should be noted that the Pourbaix diagram of Figure 1 displays the simple chemical system of As-O_2-H_2O at equilibrium at 25 C and 1 bar. In natural waters, an accurate Eh value is often difficult to obtain due to the chemical disequilibria of redox couples such as Fe(II)/Fe(III), As(III)/As(V), and SO_4^{2-}/HS^-

(Henke, 2009). As such, measured As(III)/As(V) ratios in groundwater may often be inconsistent with the predicted value from platinum electrode-derived Eh measurement (Ryu et al., 2002). In general, though, As(V) tends to be the dominant species present in oxic seawater, lakes, and river water, while ratios of As(III)/As(V) are more variable in estuaries and stratified lakes due to zones of assorted redox and salinity. Numerous factors influence the ratio of As(III)/As(V) in groundwater including redox-active solids, organic carbon, microorganism activity, and diffusion of atmospheric O_2 into soil pores (Smedley and Kinniburgh, 2002). Even the highly reducing groundwaters of Bangladesh were found to contain a wide range of As(III)/As(V) ratios from 0.1 to 10 (DPHE, 2001), emphasizing the complexity of chemical disequilibria and influence of more than simple redox conditions on arsenic speciation. This work only examines the removal of As(V), but future research should include As(III) as well.

Arsenic poisoning can occur from both acute exposure to concentrated doses of arsenic and from long-term consumption of less concentrated levels. Acute arsenic poisoning may result in vomiting, diarrhea, abdominal pain, numbness of the extremities, muscle cramps, and death in extreme cases (WHO, 2010). Long-term consumption of water with elevated levels of arsenic can lead to arsenicosis, a collection of diseases associated with exposure to arsenic over a duration of time. Changes to the skin are typically the first notable signs of arsenicosis, including hyperpigmentation, skin lesions, and hard patches on the palms and soles of the feet. Other conditions include hyperkeratosis, gangrene, renal failure, enlarged liver, high blood pressure, cardiovascular disease, peripheral neuropathy, and gastrointestinal effects (van Halem, 2009; WHO, 2010). Arsenic consumption has also been shown to cause several forms of

cancer including skin, lung, and bladder cancer. As such, arsenic has been classified by the International Agency for Research on Cancer as a Group I carcinogen (IARC, 2004).

Freshwater contamination by arsenic is a global problem, with identified contamination sites on all inhabited continents. Over 140 million people worldwide are at risk of drinking water with As concentrations > 10 µg/L, with contamination observed in over 70 countries (Ravenscroft, 2007). More than half of countries with known arsenic contamination were discovered within the last 15 years, leading to the high probability that the arsenic problem is even more widespread, yet undiscovered. Some of the major arsenic contamination problems occur in India, Bangladesh, China, Taiwan, the United States, Mexico, Chile and other Latin American countries, as seen in Figure 2.

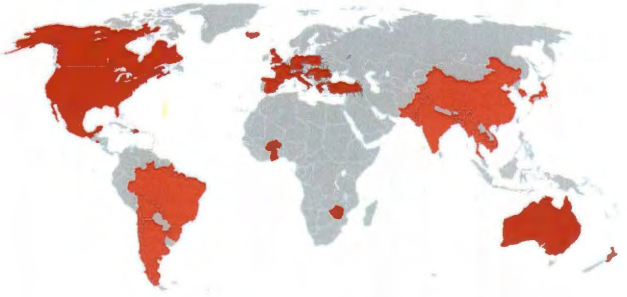

Figure 2: Nations (red) with As contaminated groundwater(van Halem, 2009)

Groundwater contamination by arsenic is also a local problem, with many water supplies affected in the United States and Mexico. Arsenic contamination is most prominent in the southwestern states, although localized problem areas are present throughout the continental US, as seen in Figure 3.

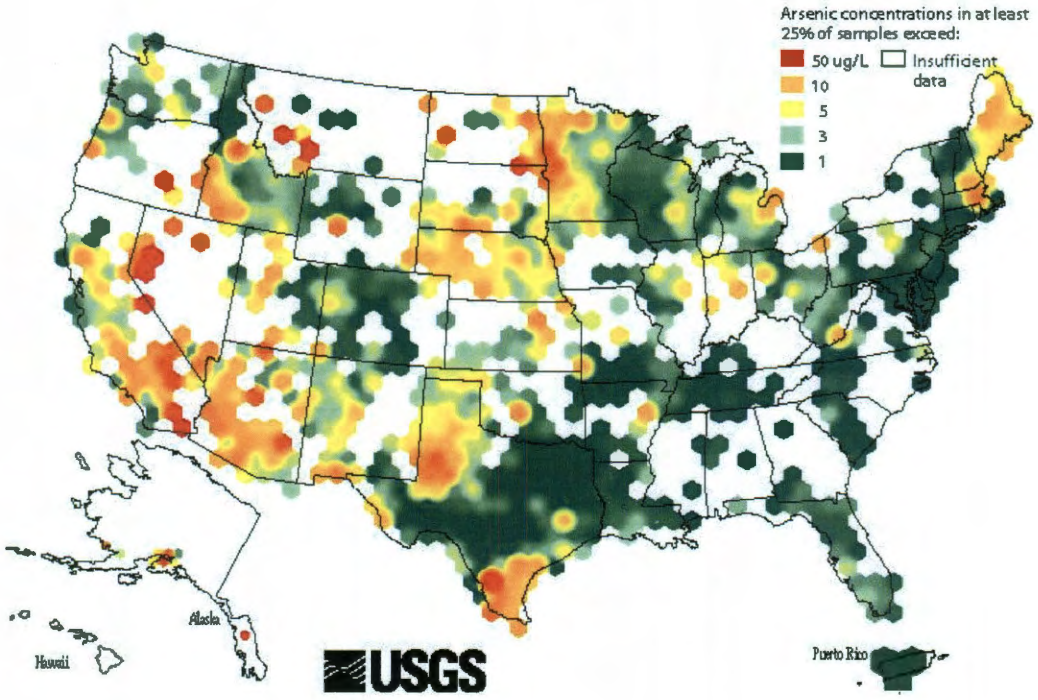

Figure 3: 75th Percentile of Arsenic contamination in US groundwater (Ryker, 2001)

Nearly 13 million people in the US alone are served by community water systems which must treat their water supplies to meet the EPA Maximum Contaminant Limit (MCL) of 10 µg/L, with 2.5 million exceeding 25 µg/L (EPA, 2001; WHO, 2001). While public water systems maintain regular sampling and treatment operations, private well owners are less likely to monitor water quality due to lack of regulation from the

EPA under the Safe Drinking Water Act. Approximately 38 million people receive water from private water wells which could contain unsafe levels of As (Bureau, 2008).

Conventional Arsenic Treatment Methods

Numerous methods have been developed and employed for the removal of arsenic from drinking water, all of which rely upon simple physical/chemical processes including adsorption, precipitation, oxidation/reduction reactions, and physical exclusion. Conventional treatment schemes identified by the US EPA include coagulation/filtration, adsorptive media, ion exchange, and membrane processes, as seen in Table 1. (EPA, 2003). Each of these technologies is appropriate for specific conditions depending upon influent water quality, water system capacity, operation and maintenance skill required, and initial capital investment.

Table 1: Advantages and disadvantages of conventional arsenic treatment processes (EPA, 2003)

Technology	Advantages	Disadvantages
Coagulation/ Filtration	No water loss Cost-effective for centralized systems	High operational skill needed
Adsorptive Media	High removal efficiency Low operational skill	Competitive interference
Ion Exchange	High removal efficiency	High operational skill needed Competitive interference
Membrane Processes	High removal efficiency Effective in most water quality conditions	High water loss High cost

Conventional coagulation/filtration involves the agglomeration of colloidal particles into large floc which can be removed by clarification or filtration through a

porous medium. The primary coagulants used for arsenic removal consist of iron and aluminum salts, which hydrolyze into relatively insoluble amorphous hydrous ferric oxide (HFO) and hydrous aluminum oxide (HAO), respectively. As(V) removal is generally much more effective than As(III) due to the removal mechanism dependence on surface charge, whereby negatively charge As(V) ($H_2AsO_4^-$, $HAsO_4^{2-}$) preferentially adsorbs to the positive surface charge of the metal floc. Thus, preoxidation steps are necessary for As(III) treatment. Additionally, pH control may be required for optimal treatment using alum (pH 5 to 7) or ferric salts (pH 5 to 8) in order to maintain positive surface charge as well as particle stability (EPA, 2003). Coagulation/filtration treatment is effective for arsenic problems in large scale water distribution system, but is inefficient for small systems and private water wells.

Arsenic sorption to a media phase is another widespread treatment method, with the most common media being activated alumina and iron based sorbents. In this process, the raw or pretreated water is passed through a bed of porous media where the arsenic is removed from solution to the solid phase through adsorption. Activated alumina is a coarse medium of Al_2O_3 with very high surface area (200-300 m^2/g) which provides a large number of sorption sites (WHO, 2001). Optimum removal occurs at pH 5.5-6.0 due to the positive surface charge of activated alumina below its PZC of 8.2 and low concentration of competing acid anions (Clifford, 1999). Preferential adsorption of common water constituents follows OH^-> $H_2AsO_4^-$> $Si(OH)_3O^-$> F^-> $HSeO_3^-$> TOC > SO_4^{2-}> H_3AsO_3; thus, preoxidation is usually required for As(III) removal due to its neutral charge in typical groundwater conditions of pH<9.2.

Common iron-based sorbents include goethite(α-FeOOH), ferrihydrite(HFO), hematite(α-Fe_2O_3), and magnetite(Fe_3O_4) which differ in oxidation state and structural arrangement. The specific surface area of goethite, hematite, and magnetite ranges from 5-200 m^2/g depending upon formation conditions and particle size while ferrihydrite is generally characterized as having much higher surface area of 100-700 m^2/g due to its poorly crystalline nature (Cornell and Schwertmann, 2003). Adsorption is strongly controlled by the dissociable surface hydroxyl groups (≡FeOH) which are able to form complexes with ions in solution. As such, it is widely observed that arsenate adsorption decreases with increasing pH while arsenite is less dependent on pH due to its neutral surface charge over a much wider pH range. Thus, pH adjustment is often required to lower the pH of natural waters into a more favorable treatment range. It has also been shown that common groundwater constituents such as phosphate, bicarbonate, and silica significantly reduce arsenic adsorption onto iron oxides due to competitive interference (Shipley et al., 2010; Zeng et al., 2008). The use of iron sorbents is still emerging and thus few studies have examined their effectiveness at full-scale treatment.

Ion-exchange is another effective arsenic treatment process by which ions are removed from the solution phase by exchanging onto a functionalized polymer resin. Arsenic removal may occur through the use of a strongly basic anion exchange resin, typically a quaternary amine, which is loaded with either chloride or hydroxide ions. Influent water is passed through the resin where the arsenic exchanges with the preloaded anions. Ion exchange efficiency is dependent upon pH and concentration of competing ions, with preferential selection according to $SO_4^{2-} > HAsO_4^{2-} > NO_3^-$, $CO_3^{2-} > NO_2^- > Cl^-$ (Clifford, 1999). Preoxidation is required for As(III) removal due to neutral molecule

charge in the typical natural water pH range. The exchange resin must be regenerated with brine backwash, which typically produces a concentrated hazardous waste stream which must be disposed of.

Membrane processes used to remove arsenic from water supplies include reverse osmosis and nanofiltration, which both require high operating pressure. While membranes are highly effective at removing arsenic, they are easily fouled by other water constituents such as natural organic matter, colloids, and inorganic scale and thus usually require pretreatment (EPA, 2003). Due to the physical separation of arsenic and other water constituents from the effluent, a highly concentrated waste stream is generated which must be disposed of.

In Situ Treatment Methods

The widespread problem of groundwater and soil contamination due to anthropogenic activity has lead to the development of numerous remediation processes. While pump-and-treat (a common technique whereby contaminated groundwater is pumped to the surface, treated, and reinjected into the groundwater aquifer) dominated remediation design of the past century, current studies have determined that this method is highly expensive and often futile in long-term cleanup success (DOD, 1998; NRC, 1994). More promising techniques developed treat the contamination *in situ*, generally resulting in less operation & maintenance cost as well as less hazardous waste generation.

Of *in situ* processes developed, permeable reactive barrier (PRB) technology has attracted some of the most interest due to high effectiveness and passive treatment once installed. Permeable reactive barriers (example seen in Figure 4) have been described as

"an emplacement of reactive media in the subsurface designed to intercept a contaminated plume, provide a flow path through the reactive media, and transform the contaminant(s) into environmentally acceptable forms to attain remediation concentration goals down-gradient of the barrier (EPA, 1989)."

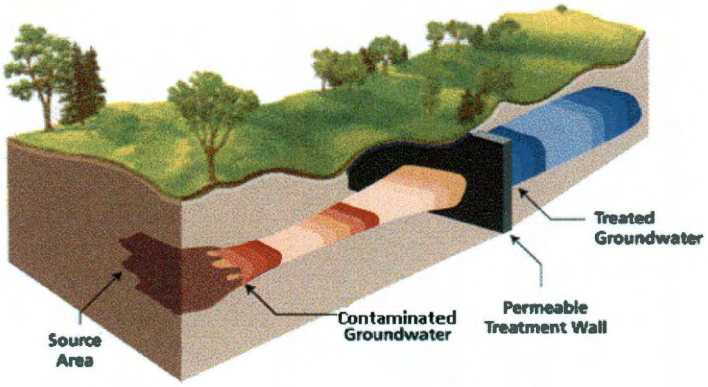

Figure 4: Conventional permeable reactive barrier treatment scheme (Stewart, 2009)

Conventional PRB systems are installed through excavation of surface and subsurface material and emplacement of reactive media, thus they are typically limited to somewhat shallow depths of 20 m (Thiruverikatachari et al., 2008). However, some advanced PRB systems can reach deeper contamination through injection installation, in which the treatment zone is emplaced by drilling a series of bore holes and injecting the reactive media into the subsurface. Several PRB technologies have been developed for the treatment of arsenic contaminated groundwater.

One of the most common PRB techniques for the treatment of numerous contaminants, including arsenic, is the emplacement of zero-valent iron (ZVI) media. In this technology, Fe(0) corrosion yields Fe^{2+}/Fe^{3+} depending on redox conditions and OH^- which precipitate as a variety of iron (oxy)hydroxides. The mechanisms of arsenic removal have been identified as both co-precipitation with and sorption onto the iron

corrosion products (Gibert et al., 2010). While this method can be highly effective for arsenic removal from groundwater, its use is limited due to excavation requirements and must be physically replaced with new ZVI once media exhaustion has occurred.

Bioremediation of contaminated soils and groundwater is another *in situ* treatment technology considered for arsenic contamination. One process involves biosorption, in which arsenic is directly adsorbed by microbial biomass as well as sorption and coprecipitation with biogenic iron (oxy)hydroxides (Wang and Zhao, 2009). Microbially facilitated oxidation/reduction processes have been shown to greatly enhance arsenic removal from groundwater through its immobilization in freshly formed Mn/Fe hydroxides and sulfides. Phytoremediation is another bioremediation technology that has shown promise for groundwater treatment, in which the soluble arsenic is removed from solution through phytoextraction, and accumulated in the plant biomass (Wang and Zhao, 2009). While bioremediation is attractive for its low cost and minimal waste generation, there are several drawbacks including that hyperaccumulating plants must be harvested and disposed of properly and the long-term fate of biosorbed arsenic is unknown. As of yet, bioremediation studies have focused on bench-scale experiments under well defined conditions, whereas actual field demonstrations are needed to demonstrate the sustainability of *in situ* arsenic bioremediation.

Carbonate Significance in Arsenic Affected Aquifers

An innovative remediation scheme based upon exchanging carbonate minerals into more reactive media for arsenic removal could be potentially significant due to the ubiquity of carbonate minerals in soil environments. Calcite and dolomite occur in a wide variety of soils, but are most commonly found in sub-humid to arid regions (Dixon

et al., 1989). Carbonate minerals in soil originate from a variety of sources including weathering of parent carbonate material, dissolution of Ca-bearing minerals, mineralization of plant materials, and mixing of rain, surface, and ground water which result in supersaturation of $CaCO_3$ (Dregne, 1976). When carbonates represent 1% or more of total noncarbonate sedimentary rocks and arid-climate soils, they tend to dominate the soil and groundwater chemistry due to high reactivity and buffering capacity (Langmuir, 1997). Thus, carbonate minerals are not only ubiquitous in the soil environment but also significantly impact the local geochemistry.

Carbonate aquifers also supply a large fraction of the world's potable water supply, with roughly 20-25% of the global population obtaining their water from karst formations (Ford and Williams, 2007). Karst is a general term encompassing soluble mineral formations, composed primarily of gypsum and limestone, of which carbonate karst occurs over 10-15% of continental land mass, as seen in Figure 5 (Ford and Williams, 2007).

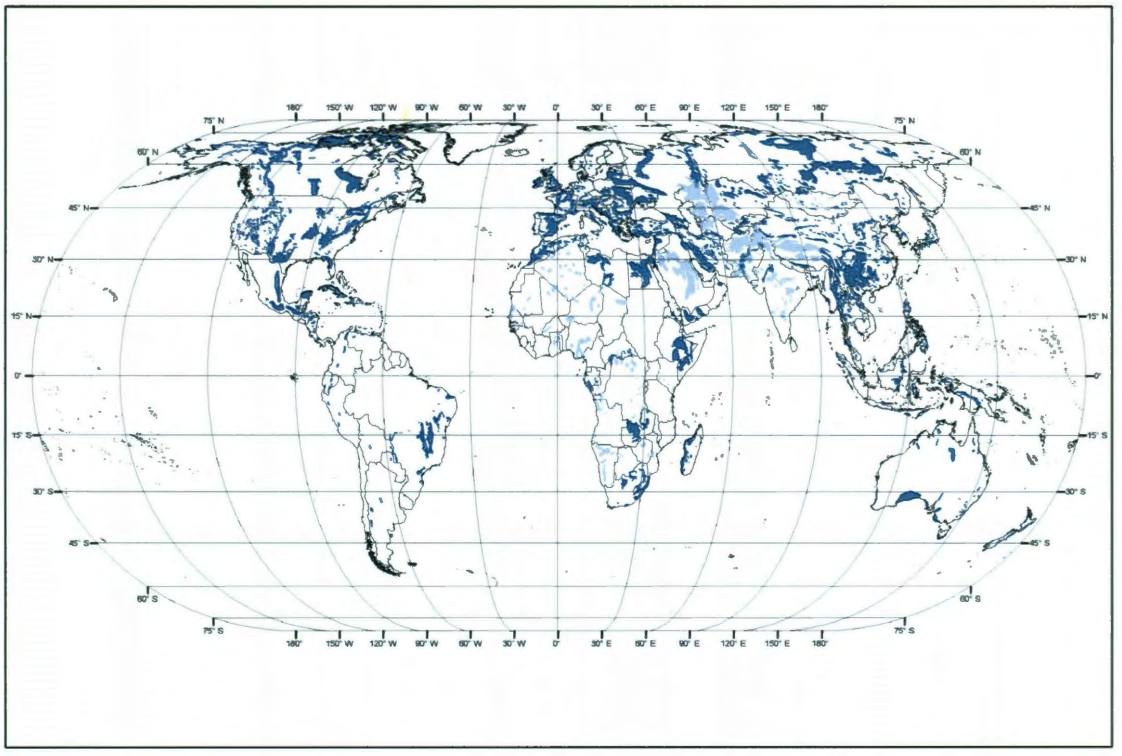

Figure 5: Global distribution of carbonate rock outcrops (Pure carbonates in dark blue and discontinuous or impure carbonates in light blue) (Ford and Williams, 2007).

Numerous arsenic affected groundwaters have been described in the literature as being at saturation equilibrium with respect to calcite, including the Pampa aquifers of Argentina (Smedley et al., 2002), the Bangladesh-Bramapoutre delta upper aquifers (Kinniburgh and Smedley, 2001), the Zimapan limestone aquifer of central-eastern Mexico (Romero et al., 2004), and the calcareous bedrock aquifer of eastern New England (Ayotte et al., 2003).

Due to the prevalence of elevated arsenic levels in New England regional water sources, a case study compared the two primary aquifer types of eastern New England: 1)unconsolidated aquifers composed mainly of sand and gravel and 2)fractured

crystalline-bedrock aquifers. Groundwater from the bedrock aquifers containing between 5-50% calcite contained significantly higher concentrations of arsenic, with nearly 1/3rd of wells having >10 μg/L As (Ayotte et al., 2003). This number is even more disconcerting considering that nearly 20% of all New England drinking water is supplied by private wells drawing from bedrock aquifers.

Arsenic contamination is also widespread throughout a 7,000 km^2 sampling region of La Pampa province in central Argentina, with 95% and 73% of samples exceeding 10 μg/L and 50 μg/L As, respectively (Smedley et al., 2002). The coarse grained aquifer mineralogy is dominated by silicates such as feldspar and quartz, with variable amounts of calcite. Secondary $CaCO_3$ is also abundant throughout the aquifer in the form of cemented nodes and layers. Due to neutral to slightly alkaline pH (7.0-8.7) and oxidizing redox potentials (131-492 mV) throughout the aquifer, Smedley et al. concluded that the high dissolved As concentrations were due to release from Fe or Mn oxides (2002). While metal (oxy)hydroxides are typically considered to control As mobilization in oxidizing conditions, the As is less strongly bound at higher pH values (8-9.5) due to electrostatic repulsion (Dzombak and Morel, 1990). Thus, similar oxidizing groundwaters with elevated pH would be ideal candidates for a carbonate exchange remediation design due to high As mobility.

Centuries of mining activity have also polluted the groundwater near Zimapan, Mexico, in both the deep fractured limestone aquifer and shallow coarse-grained conglomerate aquifer (Romero et al., 2004). Groundwater sampling found As concentrations as high as 0.437 mg/L in shallow-dug wells and 1.09 mg/L in the deep limestone wells, both of which supply the town with drinking water. While the authors

found that the calcite component of the aquifer matrix has an important role in controlling the mobility of As in local groundwater, the prevalence of carbonate-rich material provides potential for a remediation scheme based upon exchange of carbonate minerals.

Aquifer sediments of the highly As contaminated Indian subcontinent including West Bengal, India and Bangladesh have also shown to contain a considerable fraction of carbonate minerals. One local sampling of groundwater samples from West Bengal contained mean As concentrations of 75 μg/L (480 μg/L maximum) while being at local equilibrium with respect to rhodocrosite, calcite, and dolomite (Nath et al., 2009). XRD analysis of the unconsolidated sand aquifer sediment from these locations confirmed the presence of 5-10% carbonates.

Each of these examples of arsenic-affected aquifers demonstrate not only the need for a treatment scheme, but the potential of a carbonate exchange remediation design. Carbonate minerals are ubiquitous in the subsurface environment, increasing the usefulness of a remediation design which takes advantage of their presence.

Mineral Dissolution & Precipitation

Since the mechanism of *in situ* treatment discussed here involves an exchange of mineral forms in the porous media, a discussion of inorganic salt solubility is necessary. Solubility refers to the limiting amount of dissolved constituents of a solid phase under a certain set of environmental conditions, which can be reduced to a solubility product, K_{sp}. For calcite system equilibrium, the following dissolution reaction can be followed

$$CaCO_3(s) = Ca^{2+} + CO_3^{2-} \tag{1}$$

The solubility product, $K_{sp,\,Cal}$, of calcite dissolution is defined as

$$K_{sp,Cal} = \{Ca^{2+}\}_{eq}\{CO_3^{2-}\}_{eq} \tag{2}$$

Where

$(Ca^{2+})_{eq}$ = equilibrium calcium activity for given environmental conditions

$(CO_3^{2-})_{eq}$ = equilibrium carbonate activity for given environmental conditions

The thermodynamic driving force of the dissolution reaction is related to the Gibbs free energy, which is given by

$$\Delta G = RT \ln \frac{Q}{K_{sp}} \tag{3}$$

Where

ΔG = Gibbs free energy of reaction (J mol^{-1})

R = universal gas constant (8.314 J $mol^{-1}K^{-1}$)

Q = reaction quotient

For any specific chemical reaction to proceed thermodynamically, the Gibbs free energy of the overall reaction must be negative (-), whereas a Gibbs free energy of positive (+)

value would cause the reaction to be thermodynamically favorable in the reverse direction. A Gibbs free energy of zero (0) occurs for a reaction at equilibrium. Substituting the actual values of the reaction quotient into the above equation,

$$\Delta G = RT \ln \frac{\{Ca^{2+}\}_{act}\{CO_3^{2-}\}_{act}}{\{Ca^{2+}\}_{eq}\{CO_3^{2-}\}_{eq}} = RT \ln \frac{IAP}{K_{sp,Cal}} \tag{4}$$

Where

$(Ca^{2+})_{act}$ = actual calcium ion activity in solution

$(CO_3^{2-})_{act}$ = actual carbonate ion activity ion in solution

IAP = ion activity product

Thus, the ion activity product to solubility product ratio can be used to determine the direction of the Gibbs free energy and whether dissolution or precipitation of the calcite solid is thermodynamically favorable. Three conditions are possible for the thermodynamic favorability of this reaction:

$$IAP > K_{sp},\ \Delta G > 0,\ \textit{precipitation favorable}$$

$$IAP < K_{sp},\ \Delta G < 0,\ \textit{dissolution favorable}$$

$$IAP = K_{sp},\ \Delta G = 0,\ \textit{reaction at equilibrium (no net dissolution or precipitation)}$$

Similarly, the dissolution reaction of the zinc carbonate mineral smithsonite ($ZnCO_3(s)$) follows

$$ZnCO_3(s) = Zn^{2+} + CO_3^{2-} \tag{5}$$

The solubility product of smithsonite dissolution is defined as

$$K_{sp,Smith} = \{Zn^{2+}\}_{eq}\{CO_3^{2-}\}_{eq} \tag{6}$$

A comparison of several carbonate mineral solubility products allows for an understanding of the thermodynamic favorability for each solid to form in a mixed solution as seen in Table 2.

Table 2: Solubility products of common carbonate minerals

Mineral	Formula	pK_{sp}	Reference
Magnesite	$MgCO_3$	7.93	(Koziol and Newton, 1995; Wagman et al., 1982)
Calcite	$CaCO_3$	8.48	(Nordstrom et al., 1990)
Witherite	$BaCO_3$	8.56	(Nordstrom et al., 1990)
Strontianite	$SrCO_3$	9.27	(Nordstrom et al., 1990)
Siderite	$FeCO_3$	10.59	(Preis and Gamsjager, 2001)
Smithsonite	$ZnCO_3$	10.9	(Preis and Gamsjager, 2001)
Otavite	$CdCO_3$	12.01	(Preis and Gamsjager, 2001)
Cerrusite	$PbCO_3$	13.20	(Smith, 2001)

Due to the ubiquity of calcium and magnesium in nature, other carbonate minerals generally reach equilibrium in systems presaturated with calcite and/or dolomite. The low solubility of other metal carbonates relative to calcite limits their concentrations in groundwater to trace amounts (Langmuir, 1997). Assuming equilibrium between calcite and smithsonite, the following reaction equation may be followed

$$CaCO_3(s) + Zn^{2+} = ZnCO_3(s) + Ca^{2+} \quad (7)$$

The equilibrium constant of this reaction may be reduced to the solubility products of these minerals.

$$K_{eq} = \frac{\{ZnCO_3(s)\}\{Ca^{2+}\}}{\{CaCO_3(s)\}\{Zn^{2+}\}} = \frac{K_{sp,calcite}}{K_{sp,smithsonite}} = \frac{\{Ca^{2+}\}}{\{Zn^{2+}\}} \quad (8)$$

Thus, the ratio of free metal ions in solution can be correlated to the solubility products of the two minerals at equilibrium. Taking the value of $K_{sp,calcite} = 10^{-8.48}$ and $K_{sp,smithsonite} = 10^{-10.9}$ and assuming equal ion activity coefficients, the ratio of $[Ca^{2+}]/[Zn^{2+}] = 263$ in solution at equilibrium with both calcite and smithsonite.

The lower solubility of other metal carbonates may be used advantageously to exchange typical aquifer minerals, such as calcite or dolomite, into carbonate minerals with greater capacity for contaminant removal. A mineral exchange reaction can be induced by increasing the concentration of free exchange metal above equilibrium value, thus shifting equation 7 to the right. In this example, addition of free Zn^{2+} to solution will result in the thermodynamically favorable precipitation of $ZnCO_3$.

In situ Exchange Selection

PRB technology has received significant interest in the recent past due to low cost-benefit ratio and effectiveness for treating otherwise hard to remove contaminants. The EPA Remedial Technology Development Forum (RTDF) has established several criteria for successful reactive media. These desired characteristics include compatibility with the subsurface environment, long duration of reactivity, minimal impact on groundwater flow, and high worker safety (RTDF, 1998). For a sustainable remediation approach, selection of an appropriate exchange reaction must also consider the long-term environmental implications of the resulting precipitate.

The long-term stability of the exchanged aquifer media is crucial to the success of sustainable remediation design. The selected exchange precipitate must have a lower solubility than the primary aquifer mineral, in this case calcite, in order to discourage dissolution after the initial exchange. Therefore, a successful candidate mineral should have a lower K_{sp} than that of calcite ($K_{sp} = 10^{-8.48}$).

As the ultimate objective of an *in situ* groundwater remediation process, the fundamental characteristic of a designed exchange precipitate is a high capacity for contaminant removal. Similar to other PRB technologies, the media may reduce groundwater contaminants through mechanisms of sorption, oxidation/reduction, or precipitation (Gibert et al., 2010; Wang and Zhao, 2009). At a minimum, the resulting mineral should possess a greater removal capacity than the native aquifer media.

A sustainable remediation design must also consider the environmental impact of the exchange reaction and possible implications of the resulting precipitate. Overall environmental impacts must consider both the risks to human health as well as biota. The exchange precipitate should avoid solids containing toxic substances which could pose a high risk due to leaching into groundwater. While several carbonate minerals of heavy metals have intrinsically low solubility (Table 2), their regulation in drinking water due to health effects negates other advantages. The EPA regulates Ba^{2+}, Cd^{2+}, and Cu^{2+} in drinking water at an MCL of 2, 0.005, and 1.3 mg/L, respectively (EPA, 2009). Thus, the selected carbonate mineral should contain only nontoxic elements, which could be subject to human consumption in the event of leaching into groundwater.

Zinc carbonate is an ideal candidate for *in situ* exchanged media due to its low solubility and nontoxic nature of zinc. The solubility of $ZnCO_3$ ($K_{sp} = 10^{-10.9}$) is over two

orders of magnitude less than that of $CaCO_3$ ($K_{sp} = 10^{-8.48}$). Additionally, Zn^{2+} is nontoxic and only listed under the non-mandatory guidelines of secondary standards for drinking water at 5 mg/L due to metallic taste above this concentration (EPA, 2009). These characteristics are beneficial for an exchanged reactive media; however, little is known regarding the sorption characteristics of $ZnCO_3$ for contaminant removal from groundwater.

An extensive literature review found no direct studies on the use of smithsonite, hydrozincite ($Zn_5(CO_3)_2(OH)_6$) , or any other zinc carbonate solids for treatment of arsenic contaminated waters. However, zinc has been shown to enhance arsenic adsorption to the iron oxides magnetite and goethite (Grafe et al., 2004; Yang et al., 2010). Grafe found that in solution undersaturated ($IAP/K_{sp}<1$) with respect to any known Zn-As solids, 0.25 mM Zn^{2+} increased As(V) sorption onto goethite above surface saturation (2004). They concluded that a koettitgite ($Zn_3(AsO_4)_2 \cdot 8H_2O$)-like or adamite ($Zn_2AsO_4OH$)-like surface precipitate formed, providing additional surface sites for As(V) adsorption. Yang showed that concentrations as low as 1.2 mg/L Zn^{2+} significantly enhanced the kinetics and equilibrium amount of both As(V) and As(III) adsorption to magnetite nanoparticles (2010). The adsorption enhancement effect was only observed under neutral to alkaline conditions and not seen with other cations such as Ca^{2+} or Ag^{+}. Since preloaded Zn^{2+} on the nanoparticles did not increase arsenic sorption, the authors concluded that an aqueous complex such as $ZnAsO_4H_{aq}$ was first formed which may have a stronger affinity for the magnetite surface sites. These findings demonstrate that a $ZnCO_3$ remediation strategy may successfully remove arsenic from groundwater through the adsorption/surface precipitation of a Zn-As complex.

Zinc Occurrence & Toxicity

Zinc is a metallic element with atomic number 30 and occurs in oxidation state of +2. As the 24th most abundant element in the Earth's crust, the average concentration of zinc is 70 mg/kg, with typical levels between 10-300 mg/kg(Malle, 1992). The most common ores of zinc are sulfides, including sphalerite (ZnS) and wurtzite ($Zn_xFe_{1-x}S$); however, zinc is found in trace amounts in most other rock forms as seen in Table 3.

Table 3: Average Concentration of Zinc in Rocks (Drever, 1997)

Rock	Zinc (mg/kg)
Granite	50
Basalt	105
Shale	95
Sandstone	16
Limestone	20

Heavy metals such as zinc can be introduced into the hydrosphere through both rock weathering and human activities. As the primary ore source of zinc, sulfides can produce locally high concentrations of zinc due to their rapid weathering. Mining activities also contribute to acutely elevated levels of zinc in waters due to the exposure of previously concealed rocks as well as the oxidation of sulfide minerals and subsequent dissolution.

Due to the introduction of zinc into the environment as part of a remediation design in this work, it is pertinent to understand the health risks associated with its consumption. Zinc is an essential trace nutrient necessary for the growth, development,

and health maintenance of all animal species including humans. As such, both inadequate and excessive doses of zinc can result in human health effects(EPA, 2005).

Numerous studies have reported on the adverse effects of both acute and long-term zinc toxicity. The primary health concern from excessive oral zinc exposure is that of decreased copper levels in the body arising from diminished copper absorption. Low systemic copper levels can lead to a variety of health effects including decreased copper metalloenzyme activity, decreased cholesterol levels, immunotoxicity, and gastrointestinal problems(EPA, 2005).

Several dose-response studies have established Lowest-Observed-Adverse Effect Levels (LOAEL) for zinc based upon the minimum concentration of zinc necessary to induce a negative physiological response. The Joint FAO/WHO Expert Committee on Food Additives first established a provisional maximum tolerable daily intake of 1.0 mg/kg body weight(Joint FAO/WHO Expert Committee on Food Additives., 1982) which is still the accepted standard of the WHO(WHO, 2011). Other researchers have observed similar LOAELs between 0.81 and 0.99 mg/kg-d (Fischer et al., 1984; Milne et al., 2001; Yadrick et al., 1989). The EPA has established a risk-based LOAEL of 0.91 mg/kg-d as the toxicological standard of oral zinc exposure(EPA, 2005). There is no established MCL for zinc due to its low prevalence in water sources; however, a secondary drinking water standard of 5 mg/L exists for aesthetic purposes (CITE EPA).

While harm may certainly occur from excessive consumption of zinc, it is also pertinent to understand the health hazards associated with insufficient dietary zinc intake. Zinc is necessary for the proper function of over 300 enzymes including some essential to cell replication such as DNA polymerase and reverse transcriptase(EPA, 2005). The

major function of zinc in these enzymes includes participation in catalysis reactions, regulatory function, and maintenance of structural stability. Severe zinc deficiency can result in diarrhea, mental disturbance, alopecia, and impaired cell-mediated immunity, while moderate zinc deficiency can cause growth retardation, skin changes, poor appetite, male hypogonadism, mental lethargy, and delayed wound healing(Sandstead, 1994; Walsh et al., 1994). Taking into consideration the essential nature of zinc for numerous physiological processes, the WHO established a daily dietary requirement of 0.3 mg/kg zinc (WHO, 2003).

Column Adsorption & Transport Modeling

The significant interfacial phenomenon of adsorption is pertinent to many applications in environmental engineering, not least of which is water treatment. Adsorption of ions from solution occur due to several forces including chemical, electrostatic, and van der Waals forces. While chemical forces usually occur only across short distances due to the merging of electron clouds for covalent bonding, electrostatic forces can be felt over longer distances (Stumm and Morgan, 1996). The van der Waals energy of interaction is always attractive; however, it is much smaller in comparison to covalent bonding or electrostatic interaction. Since the expected mechanism of arsenic removal in this work is due to adsorption onto the exchanged aquifer media, the solute transport can be modeled as flow through porous media. The adsorption of ions from solution flowing through a porous medium is controlled by four mass transfer processes (Seader et al., 2011):

1. Bulk solution transport- solute transport by convection and dispersion through interparticle pore space
2. External film transport- solute transport from bulk flow to outer perimeter of particle through particle boundary layer
3. Internal pore transport- solute transport by diffusion through internal pore space of particles
4. Surface diffusion & adsorption- solute transport by diffusion along particle surface and final adsorption

In ideal fixed-bed adsorption with a constant influent solute concentration, local equilibrium is achieved instantaneously between the adsorbent material and solution. This idealized transport model results in a solute "stoichiometric front" which progressively moves through the column, as seen in Figure 6, with upstream solute concentration equal to the influent concentration and upstream adsorbent completely saturated with solute.

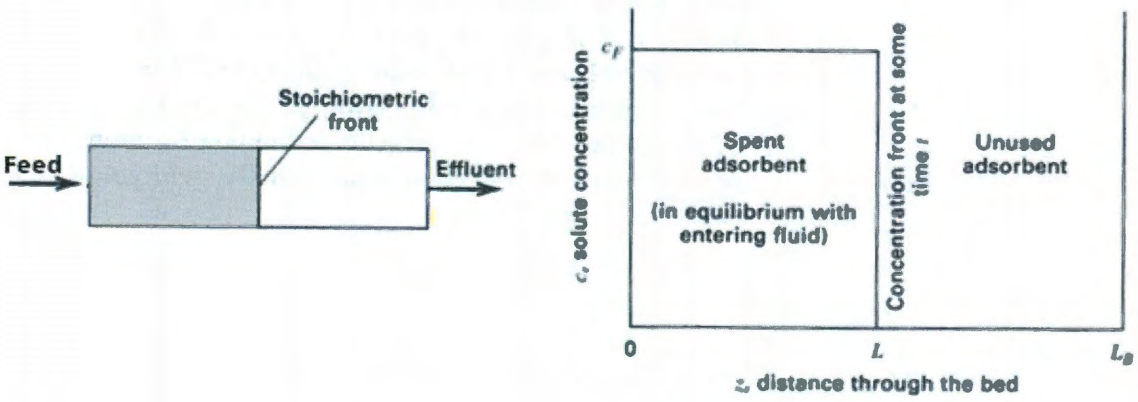

Figure 6: Stoichiometric front resulting from ideal fixed-bed adsorption (Seader et al. 2011)

This case relies on several assumptions including negligible transport resistance through external film and internal pore transport, ideal plug flow, and adsorption isotherm beginning from origin (Seader et al., 2011).

However, real fixed-bed adsorption does not follow these assumptions ideally, resulting in a non-ideal stoichiometric breakthrough front. In actual porous media systems, adsorption from solution onto the solid phase does not achieve local equilibrium instantaneously, rather adsorption occurs throughout a region of the bed known as the mass-transfer zone (MTZ). The MTZ is taken as the region between $C/C_0 = 0.05$ and $C/C_0 = 0.95$, resulting in an "S" shaped effluent breakthrough curve, as seen in Figure 7.

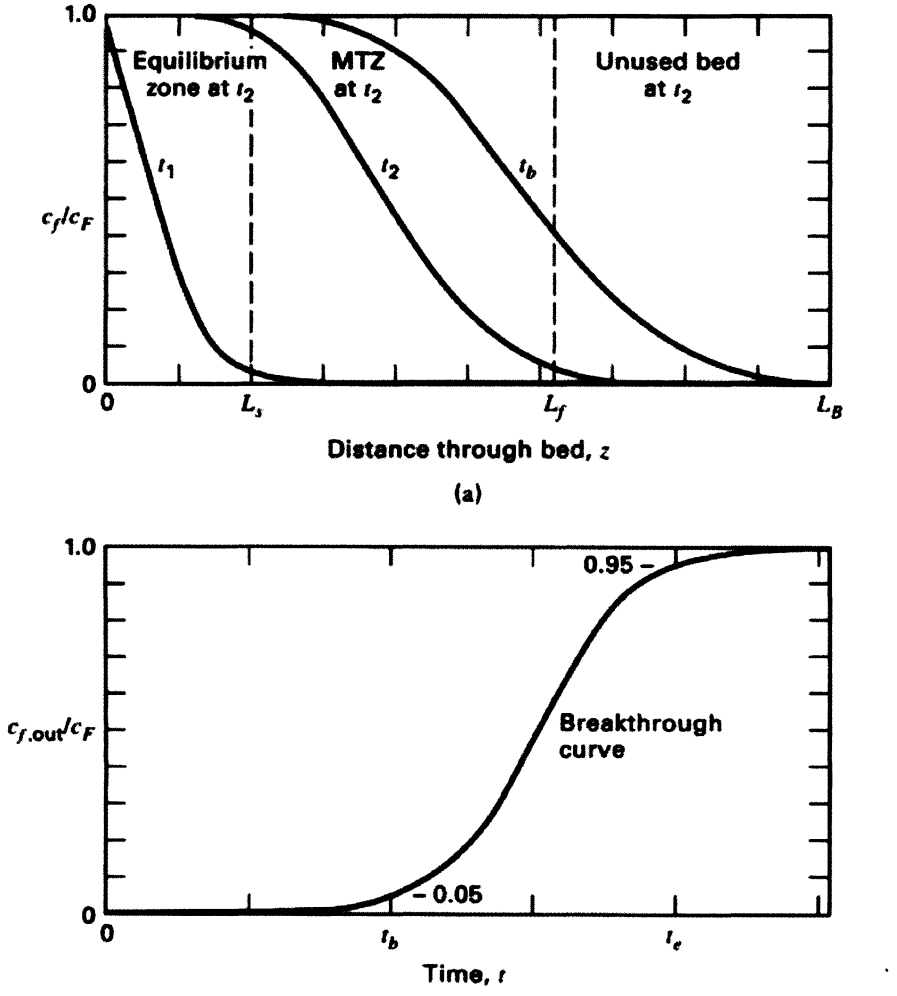

Figure 7: Mass transfer zone adsorption and effluent breakthrough curve (Seader et al. 2011)

From the example concentration profile through bed length at time t_2, the adsorbent is saturated up through distance L_s, while relatively no adsorption occurs past distance L_f. The actual solute adsorption to the media occurs in the MTZ from L_s to L_f. At time t_b, the leading front of the MTZ has reached the end of the bed, L_B, resulting in the start of the breakthrough curve for the bed effluent concentration $C_{f,out}/C_F$ vs. time plot.

In order to model solute transport in real systems, the convection-dispersion equation may be used. For one-dimensional transport of a reactive solute subject to

linear adsorption and first-order degradation in a homogeneous media under steady-state flow, the convection-dispersion equation takes the following form

$$R\frac{\partial c}{\partial t} = D\frac{\partial^2 c}{\partial x^2} - v\frac{\partial c}{\partial x} - \mu c \tag{9}$$

Where

R = retardation factor

c = solute concentration of liquid phase (ML^{-3})

D = dispersion coefficient (L^2T^{-1})

v = average pore-water velocity (LT^{-1})

μ = first-order decay coefficient (T^{-1})

Two main assumptions are taken into account for the above equation: linear adsorption coefficient and local partitioning equilibrium achieved between the solute and adsorbed phase. The retardation factor is a common term used to describe the impact of sorption on the transport of a solute and relate its movement through a phase to that of the carrier fluid. In the case of solute transport in groundwater, R can be defined as the ratio of water transport rate to that of solute transport rate, or

$$R = 1 + \frac{\rho_b K_d}{\theta} \tag{10}$$

Where

ρ_b = porous media bulk density (ML^{-3})

K_d = solid-liquid distribution coefficient for linear adsorption (L^3M^{-1})

θ = saturated volumetric water content, or void fraction (L^3L^{-3})

It should be noted that a linear adsorption ratio (K_d) must be assumed to solve Equation 9 analytically. Although many adsorption isotherms are actually nonlinear in nature, the assumption of linearity is made for the analytical solution and may be a potential source of error.

Additionally, the assumption of local equilibrium is not always true due to kinetic effects on partitioning. The actual adsorption process has been modeled as a combination of two sorption sites, with adsorption on some sites instantaneous, and adsorption on other sites following first-order kinetics (Cameron and Klute, 1977). Combining the definition of R and the concept of two site adsorption into the convection-dispersion equation, a two-site nonequilibrium model for steady state flow in homogeneous media follows (Toride, 1995).

$$\left(1+\frac{f\rho_b K_d}{\theta}\right)\frac{\partial c}{\partial t}=D\frac{\partial^2 c}{\partial x^2}-v\frac{\partial c}{\partial x}-\frac{\alpha\rho_b}{\theta}\left[(1-f)K_d c-s_k\right]-\mu_l c-\frac{f\rho_b K_d \mu_{s,e} c}{\theta} \tag{11}$$

$$\frac{\partial s_k}{\partial t}=\alpha\left[(1-f)K_d c-s_k\right]-\mu_{s,k}s_k \tag{12}$$

Where

f = fraction of exchange sites always at equilibrium

α = first order kinetic rate coefficient (T^{-1})

s_k = concentration of adsorbed phase on kinetic sites (MM^{-1})

μ_l = first-order decay coefficient for the liquid phase (T^{-1})

$\mu_{s,e}$ = first-order decay coefficient for adsorbed phase on equilibrium sites (T^{-1})

$\mu_{s,k}$ = first-order decay coefficient for adsorbed phase on kinetic sites (T^{-1})

Terms in the two-site nonequilibrium convection-dispersion equation represent, from left to right, equilibrium site retardation, dispersion, convection, transfer of solute to kinetic sites, liquid phase solute decay, and equilibrium site solute decay. Terms in the second differential equation represent change in concentration of solute adsorbed to kinetic sites, transfer of solute to kinetics sites, and decay of solute adsorbed on kinetics sites. This work utilizes the software CXTFIT to simultaneously solve the differential equations above for an accurate estimation of relevant transport parameters. CXTFIT is a commonly employed software code using a nonlinear least squares fit method to solve the convection-dispersion equation with user-defined parameters(Parker, 1984; Toride, 1995).

3. Materials and Methods

Experimental Solutions

Experiments were performed in one of two solutions: buffered electrolyte solution or Rice groundwater. Buffered electrolyte solution was composed of 5 mM NaCl with 5 mM tris(hydroxymethyl)aminomethane (TRIS) adjusted to pH 8.0 with Trace Metal Grade (TMG) HNO_3, except where noted. This solution was made from ultrapure laboratory water deionized by a reverse osmosis membrane followed by a 4 stage Barnstead filter (high capacity anion/cation exchange column, two ultrapure ion exchange columns, and one organics removal column). This electrolyte solution was chosen to represent a typical ionic strength and pH of groundwater. Rice groundwater was collected from the Rice University well (Evangeline aquifer, 1600 feet depth) adjacent to Mechanical Laboratory Building prior to chlorination. The groundwater was aerated and allowed to come to room temperature prior to experiments in order to prevent changes in solution conditions throughout the experiments. Rice groundwater properties can be seen in

Table 4.

Table 4: Measured properties of aerated Rice groundwater at 22 C

Property	Value	Method
pH	8.75	Orion combination electrode
Redox (mV)	190	HACH probe
Alkalinity (mg/L as $CaCO_3$)	180	HACH Phenolphthalein titration
Conductivity (uS/cm)	515	HACH probe
Chloride (mg/L)	30	HACH mercuric nitrate titration
Sodium (mg/L)	98.0	ICP-OES
Iron (mg/L)	0.09	HACH FerroVer
Calcium (mg/L)	11.2	ICP-OES
Magnesium (mg/L)	3.0	ICP-OES
Zinc(mg/L)	0.0	ICP-OES
Silica (mg/L as SiO_2)	16.5	ICP-OES

Sulfide (ug/L)	<5	HACH Methylene Blue Reagent
Sulfur (mg/L)	2.3	ICP-OES

All chemicals used in this study were ACS reagent grade from Fisher Scientific and Sigma Aldrich, unless otherwise noted. Concentrated stock solution of 1000 mg/L As(V) was prepared from arsenic(V) oxide hydrate ($As_2O_5 \cdot 3H_2O$) in 0.1 M NaOH and used to spike experimental solutions to desired As(V) concentrations.

All experiments were performed at room temperature (22° ± 1 C) unless otherwise noted.

All pH measurements were made using an Orion-Research combination glass electrode calibrated with pH 4, 7, and 10 standard solutions.

Solid Characterization

All calcite minerals used in this study were Iceland spar solids from Creel, Chihuahua, Mexico (Ward's Scientific). The rock sample was ground and sieved to 106-180 μm size range. Before use, the solids were washed 3 times with 1 mM acetic acid, then rinsed 3 times with DI water in order to remove all fines and impurities, prior to oven drying at 70 C. The washed Iceland spar surface can be seen in Figure 8.

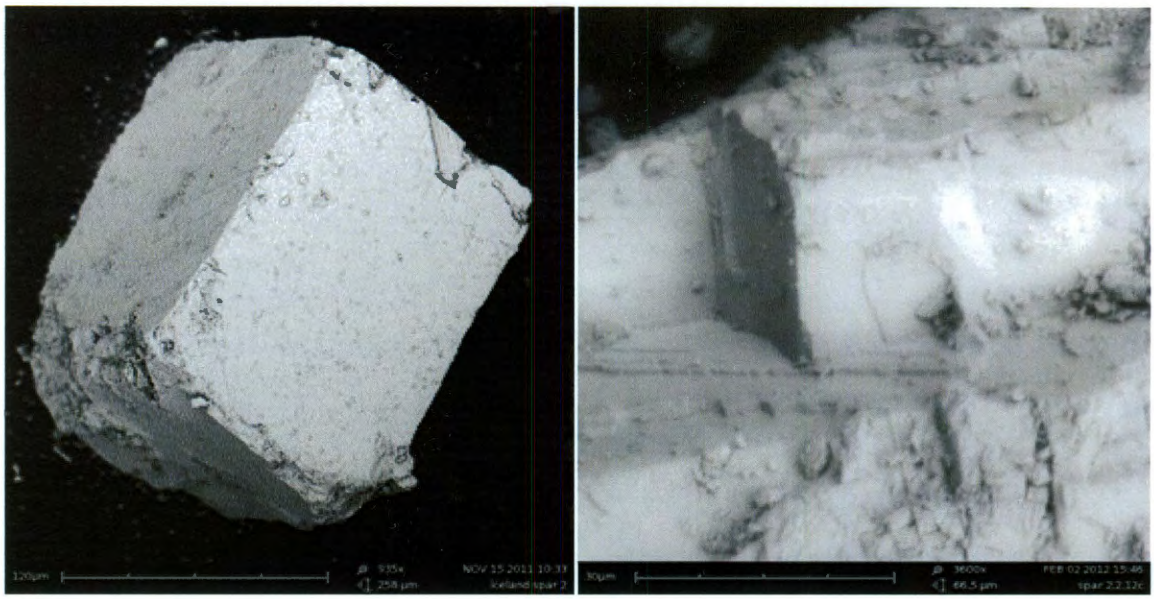

Figure 8: SEM image of washed iceland spar

The surface area of reagent grade $ZnCO_3$ was determined using BET surface area analysis with a Quantachrome Autosorb 3B Surface Analyzer (Quantachrome, Boynton Beach, Florida). To remove adsorbed moisture and gases, a known mass of $ZnCO_3$ was heated under vacuum to 100 °C for 12 hours. A multi-point adsorption-desorption nitrogen isotherm was recorded and fit to the BET isotherm, as seen in Figure 9.

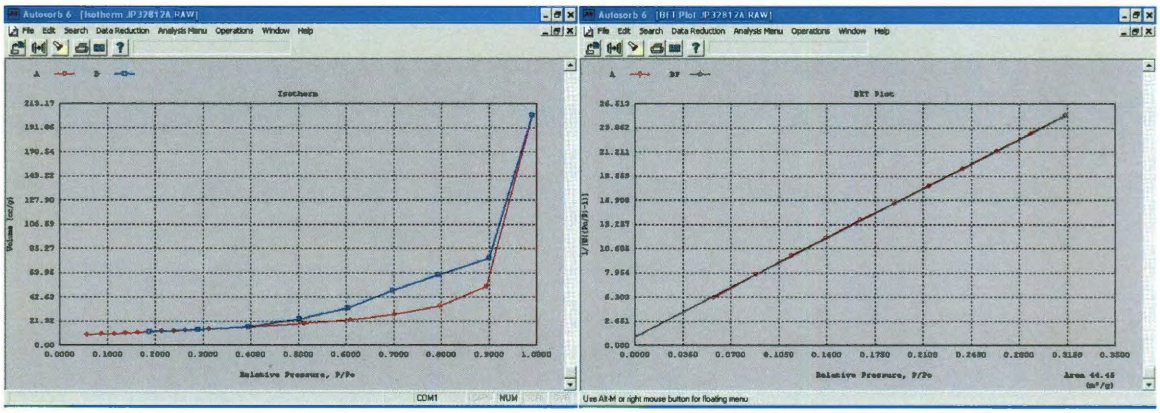

Figure 9: Nitrogen adsorption-desorption isotherm and BET plot

The fitted BET equation yielded a surface area of 44.45 m^2/g. Since adsorption-desorption hysteresis is indicative of micro- or meso-porosity (Quantachrome, 2004), the reagent grade material appears to be porous.

The precipitated zinc carbonate solids from the column exchange experiment were analyzed by X-ray diffraction (XRD) and scanning electron microscopy (SEM). XRD analysis was employed on a Rigaku D/Max Ultima II Powder Diffractometer using a Cu Kα radiation source at 40 kV and 40 mA (Rigaku, Tokyo, Japan). The resulting diffraction pattern was processed using the MDI Jade 9.4 software package (Materials Data Inc., Livermore, CA) containing the International Centre for Diffraction Data (ICDD) PDF-4+ pattern database. SEM was employed on a Phenom high resolution desktop imager with 5 kV accelerating voltage (Phenom-World, Eindhoven, the Netherlands). The zinc-exchanged calcite particles were also analyzed by BET N_2 surface analyzer which yielded a surface area of 9.78 m^2/g when fit to the BET equation.

Elemental Analysis

Arsenic was analyzed by Inductively Coupled Plasma-Mass Spectrometer (ICP-MS) in the μg/L range (Elan 9000, Perkin Elmer). Arsenic detection was normalized to a 65 μg/L Germanium internal standard in order to account for small variations in pump flowrate and sample nebulization. The ICP-MS was calibrated with a five-point calibration (0-200 μg/L As) using standards prepared from Perkin Elmer certified atomic spectroscopy standard solution. The relative standard deviation (RSD) of each measurement was typically less than 3% and correlation coefficient, R^2, greater than 0.9999. The instrument was recalibrated with new standards when $R^2 < 0.9999$.

Other metals, such as Ca^{2+} and Zn^{2+}, were analyzed by Inductively Coupled Plasma-Optical Emission Spectrometer (ICP-OES) in the mg/L range (Optima 4300, Perkin Elmer). Elemental detection was normalized to a 5 mg/L Yttrium internal standard in order to correct minute variations in pump flowrate and sample nebulization. The ICP-OES was calibrated with a three to five point calibration using standards prepared from Perkin Elmer certified atomic spectroscopy standard solution. The relative standard deviation (RSD) of each measurement was typically less than 3% and correlation coefficient, R^2, greater than 0.9999. The instrument was recalibrated with new standards when $R^2 < 0.9999$.

Adsorption Kinetics Study

In order to determine an accurate adsorption isotherm, the adsorbate is assumed to have reached equilibrium partitioning between the solid and liquid phases. The assumption of equilibrium is highly dependent on the rate of the partitioning reaction, thus the kinetics must first be understood to ensure a sufficient duration of time for the adsorption experiment to reach equilibrium. Since kinetics can be dependent on all solution components, the kinetics experiment was carried out both on a buffered electrolyte solution and solution of Rice groundwater.

The kinetics experiments were conducted in 1 liter glass bottles(Nalgene) containing either 1 liter of electrolyte solution (pH 8.0) or Rice groundwater spiked with approximately 125 μg/L As(V). The solutions were stirred continuously with a magnetic stir bar and plate to ensure completely mixed reactor. A mass of 100 mg reagent grade $ZnCO_3$ (Acros Organics) was added to each stirred reactor, and 10 mL aliquots were taken from the stirred solution at set time intervals. The samples were filtered with 0.45

μm filter to remove particulate solids and acidified to 1% HNO_3 with TMG HNO_3. Final pH of both solutions were checked to remain within ± 0.2 pH units of original pH.

Batch Adsorption Study

From batch kinetics results, >99% of As(V) adsorption to $ZnCO_3$ occurs within first 24 hours, thus all batch adsorption studies were conducted for minimum of 24 hours. A designated mass (5-100 mg) of reagent grade $ZnCO_3$ was added to 1-L glass bottle (Nalgene) containing 1 L of electrolyte solution spiked with 125 μg/L As(V). Completely mixed solution was maintained with magnetic stir bar and plate for 24 hour reaction period, after which a 10 mL aliquot was withdrawn. The sample was filtered with 0.45 μm filter and acidified with TMG HNO_3 to 1% acid for elemental analysis with ICP-MS and ICP-OES. This batch adsorption experiment was repeated with same procedure as above using Rice groundwater spiked to 125 μg/L As(V).

Similarly, a batch adsorption study was carried out using zinc-exchanged calcite particles in order to differentiate between reagent grade $ZnCO_3$ and freshly precipitated crystals. The procedure for exchange involved wet-packing a column with 106-180 μm Iceland spar particles, then pumping a 5 mM NaCl 60 mM $ZnCl_2$ solution at pH 6.0 through the column for 4500 PV. Afterwards, 10 PV of deionized water were pumped through the column to remove excess solution and the solids were dried at 100 C for 7 days.

For the batch adsorption, an assorted mass (10-110 mg) of Zn-exchanged calcite was added to 250 ml of buffered electrolyte solution spiked to 15-380 μg/L As(V). A smaller solution volume was used due to the smaller surface area of zinc-exchanged

calcite (9.78 m^2/g) compared to reagent grade $ZnCO_3$ (44.45 m^2/g). This experiment was also repeated in aerated Rice groundwater.

Column Adsorption Study

Both a buffered electrolyte solution and Rice groundwater solution spiked to 100 µg/L As(V) were fed through identical $ZnCO_3$ columns in order to determine the competitive interference from typical groundwater constituents. To demonstrate the entire remediation process of calcite aquifer media, a $CaCO_3$ packed column was first exchanged with Zn^{2+} solution before monitoring As(V) adsorption.

The Iceland spar particles were wet packed into a 6.6 mm diameter, 7 cm long borosilicate glass column with cross-sectional area of 0.3421 cm^2 (Omnifit, Bio-Chem Valve Inc., Boontoon, NJ). Deionized lab water was pumped through the column in up-flow mode at rate of 15 ml/hr while particles were added, maintaining about 0.5 cm of water depth above the particles at all time. Wet-packing the column reduces air pockets in media and helps prevent preferential flow paths from forming. The column media was tapped periodically to ensure compaction and complete packing. The Iceland spar was packed to a total length of 1 cm and capped with an adjustable plunger. A 5 mM NaCl solution was pumped through the column at rate of 10 ml/hr for minimum of 2 hours prior to any column studies in order to remove any remaining air bubbles and stabilize the media.

In order to exchange the calcite media to $ZnCO_3$, a concentrated Zn^{2+} solution was pumped through the column. A 5 mM NaCl, 60 mM $ZnCl_2$ solution was adjusted to pH 6.0 with TMG HNO_3 and pumped through the column at a flow rate of 10 ml/hr (v = 54 ft/d) with a Pharmacia P-500 syringe pump, as seen in Figure 10. The effluent pH was

monitored and samples were acidified to 1% acid with TMG HNO_3 for elemental analysis with ICP-OES. Before arsenic breakthrough solution was pumped through the column, 10 PV of 5 mM NaCl were pumped through to remove excess Zn^{2+} so that the solution would not be supersaturated with respect to any Zn-As solid phases.

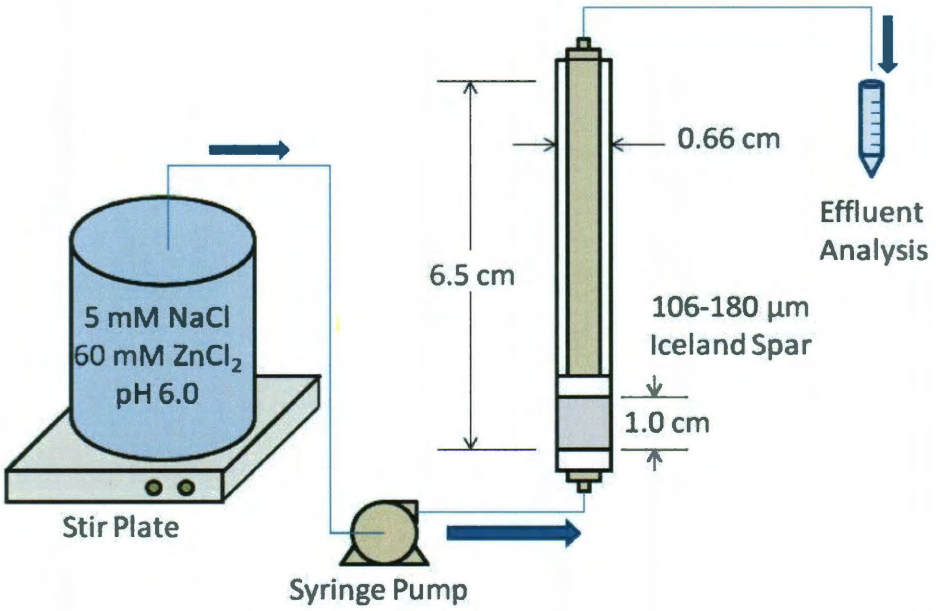

Figure 10: Column exchange apparatus design

After the exchange reaction, arsenic solution was passed through the column to monitor retardation with the precipitated media. Buffered electrolyte solution was pumped through the column with a Pharmacia P-500 syringe pump at a flow rate of 2 ml/hr (10.7 ft/d). Due to the small column pore volume, larger, multi-pore volume samples were collected and acidified to 1% acid with TMG HNO_3 for elemental analysis with ICP-OES and ICP-MS. All effluent concentrations were plotted at midpoint pore volumes of the collected sample.

Control Column Adsorption

In order to compare the zinc treatment to untreated calcite, arsenic solution was pumped through a plain calcite column as a control. Since arsenic adsorption is expected to be small relative to the treated column, greater pore volume resolution is needed for a more accurate determination of retardation factor for the calcite material. Thus, a similar experiment to the $ZnCO_3$ column adsorption was performed using a larger column for greater total pore volume.

The Iceland spar particles were wet packed into a 10 mm diameter, 10 cm long borosilicate glass column with cross-sectional area of 0.7854 cm^2 (Omnifit, Bio-Chem Valve Inc., Boontoon, NJ). Deionized lab water was pumped through the column in up-flow mode at rate of 15 ml/hr while particles were added, maintaining about 0.5 cm of water depth above the particles at all time. Wet-packing the column reduces air pockets in media and helps prevent preferential flow paths from forming. The column media was tapped periodically to ensure compaction and complete packing. The Iceland spar was packed to a total length of 10.1 cm and capped with an adjustable plunger. A 5 mM NaCl solution was pumped through the column at rate of 10 ml/hr for minimum of 2 hours prior to any column studies in order to remove any remaining air bubbles and stabilize the media.

Arsenic solution was passed through the column to monitor retardation with the precipitated media. Buffered electrolyte solution was pumped through the column with a Pharmacia P-500 syringe pump at a flow rate of 5 ml/hr (11.1 ft/d). Multi-pore volume samples were collected and acidified to 1% acid with TMG HNO_3 for elemental analysis

with ICP-OES and ICP-MS. All effluent concentrations were plotted at midpoint pore volumes of the collected sample.

Column Hydraulic Properties

Hydraulic properties of each column were evaluated using a potassium chloride tracer solution. The tracer solution consisted of the same buffered electrolyte solution used in the synthetic water experiments containing 5 mM TRIS, 5 mM NaCl with 25 mM KCl adjusted to pH 8.0 with TMG HNO_3. KCl is a common conservative tracer used in environmental column studies due to lack of reaction or sorption with calcite media (Keller et al., 2004; Pote et al., 2003). Tracer solution was pumped through each column at the same flow rate as the As(V) experiments (2 ml/hr for 0.66 cm ID columns and 5 ml/hr for 1.0 cm ID column) prior to zinc exchange solution or As(V) breakthrough solution. Effluent samples were acidified to 1% acid with TMG HNO_3 and analyzed for K^+ using ICP-OES.

The K^+ breakthrough curves of each column were fit to the 1-D convection-dispersion equation (Equation 9) using CXTFIT, as seen in Figure 11.

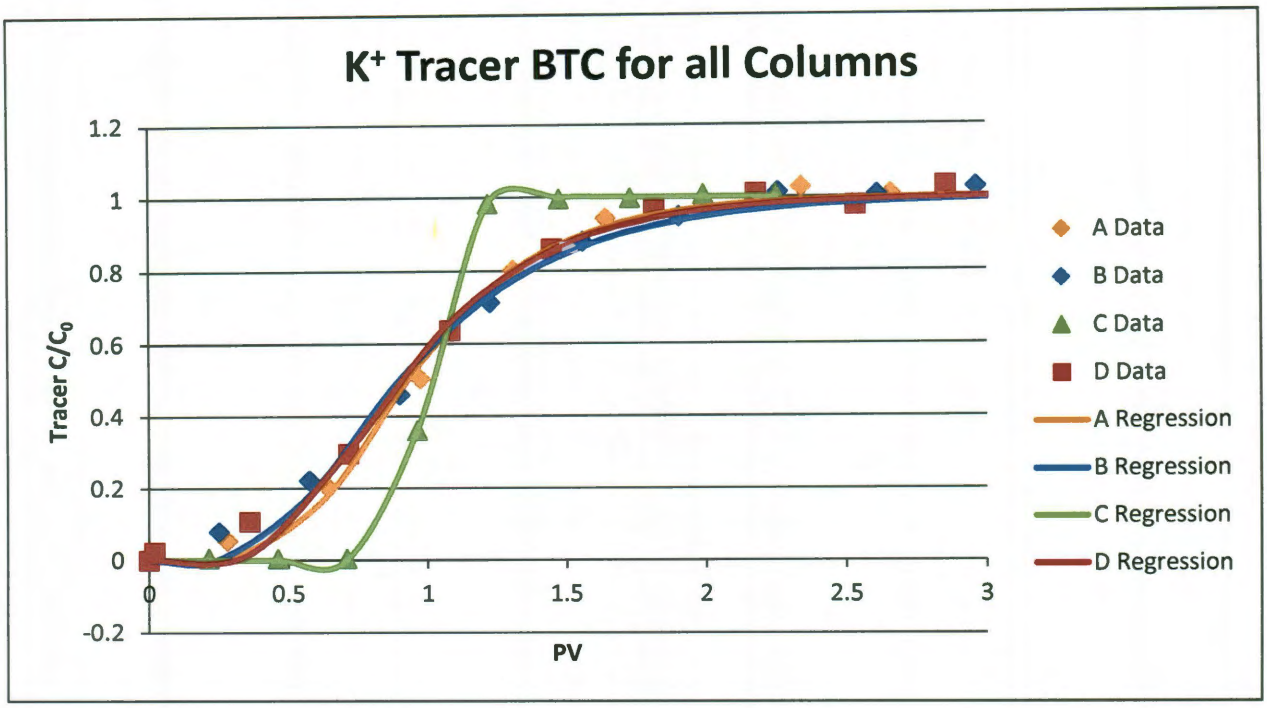

Figure 11: K^+ tracer breakthrough curves for all columns

While columns A, B, and D all exhibit similar tracer breakthrough curves, column C breakthrough is much steeper. This is likely due to the larger column dimensions and pore volume of column C, resulting in smaller relative column dead volume than the other three columns. The smaller pore volume of columns A, B, and D (0.1466 ml) is similar to the dead volume at the exit of the column (≈0.2 ml), thus greater mixing is probable. This is evident in the greater dispersion coefficients (Table 5) of the three smaller columns compared to column C as determined by CXTFIT.

Table 5: Column hydraulic property comparison from tracer experiment

Column	D (cm)	L (cm)	θ	PV (ml)	R	D (cm2/min)	R2
A	0.66	1	0.43	0.1466	1.010 ±0.022	2.01E-02 ±3.06E-03	0.994
B	0.66	1	0.43	0.1466	1.018 ±0.031	3.01E-02 ±5.32E-03	0.992
C	1.00	10.1	0.45	3.5911	1.002 ±0.002	1.07E-02 ±9.70E-04	0.999
D	0.66	1	0.43	0.1466	0.994 ±0.031	2.40E-02 ±4.93E-03	0.992

The hydraulic properties of each column were determined from the modeled fit of each tracer breakthrough curve. Using the gravimetrically determined PV from each column, an R value of 1.00 ±0.02 was obtained for each tracer breakthrough curve. The deviation in R from 1.00 is within the standard deviation for each determination, thus the gravimetric PV is verified as accurate.

The experiments run in columns A, B, C, and D were the Zn-exchanged calcite for batch As(V) adsorption, Zn-exchanged calcite synthetic water As(V) breakthrough, calcite control synthetic water As(V) breakthrough, and Zn-exchanged calcite Rice groundwater As(V) breakthrough, respectively.

4. Results and Discussion

Adsorption Kinetics

In order to determine an adequate duration for isotherm experiments, the kinetics of As(V) adsorption to reagent grade $ZnCO_3$ was first studied in both a buffered electrolyte solution and Rice groundwater. Both kinetics experiments exhibited biphasic adsorption, with very rapid adsorption in the first few hours and slow afterwards, as seen in Figure 12. The biphasic first-order kinetic model used to fit the data follows

$$\frac{C_t - C_e}{C_0 - C_e} = f * e^{-k_r t} + (1-f) * e^{-k_s t} \tag{13}$$

Where

C_t = solution concentration at time t (μg/L)

C_e = solution concentration at adsorption equilibrium (μg/L)

C_0 = initial solution concentration (μg/L)

f = mass fraction of adsorbate adsorbed rapidly

k_r = apparent rapid adsorption first-order rate constant (h^{-1})

k_s = apparent slow adsorption first-order rate constant (h^{-1})

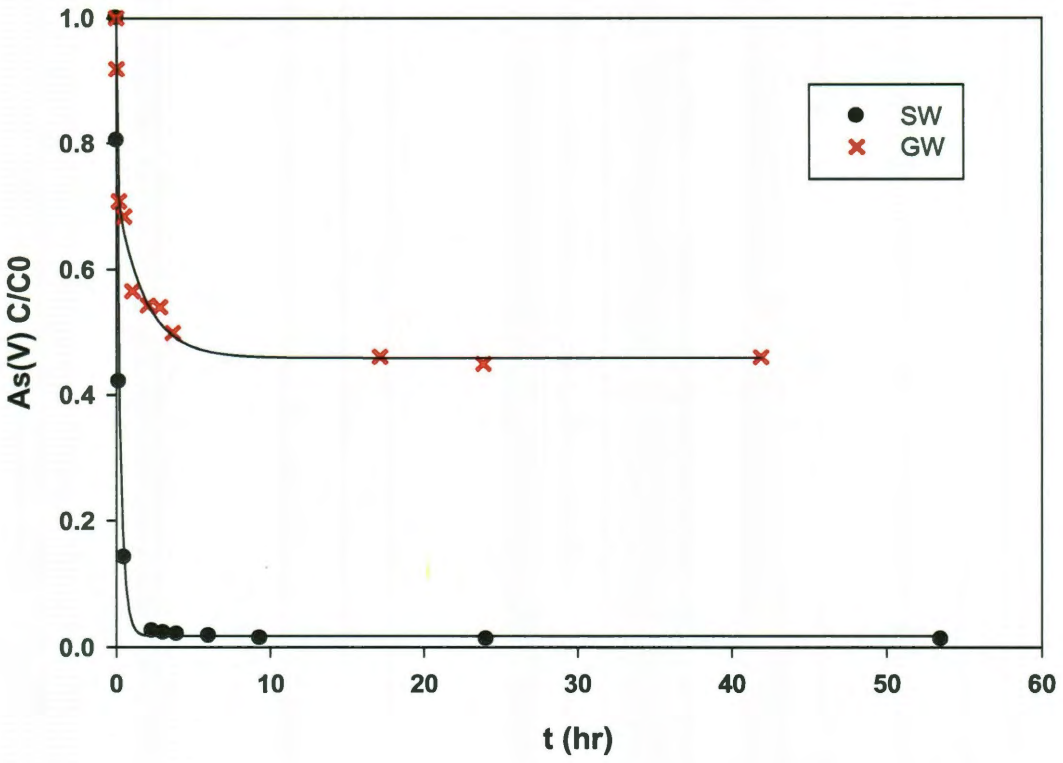

Figure 12: Adsorption kinetics of 100 ug/L As(V) onto 0.1 g/L $ZnCO_3$

Similar biphasic adsorption kinetics have been reported for arsenic adsorption onto other minerals including aluminosilicates and iron oxides (Arai et al., 2005; Raven et al., 1998; Yang et al., 2010).

Fitted model parameters for the adsorption kinetics experiments are shown in Table 6. The adsorption kinetics data fits the biphasic model very well due to its empirical nature.

Table 6: Biphasic model parameters of adsorption kinetics data

Solution	C_0 (µg/L)	C_e/C_0	f	K_r (h^{-1})	K_s (h^{-1})	R^2
SW	111	0.018±0.002	0.260±0.020	55.456±6.195	3.535±0.126	0.999
GW	168	0.459±0.012	0.515±0.046	20.267±6.944	0.546±0.111	0.991

While greater than 90% of equilibrium adsorption values (C_e/C_0) were reached within the first 3 hours for both buffered electrolyte and groundwater solutions, the groundwater solution exhibited slightly less rapid adsorption by comparison of k_r value. This could possibly be due to competitive interference from other constituents in the groundwater makeup. Both experiments achieved greater than 99.99% of their equilibrium adsorption value within 24 hours, thus this duration was chosen as sufficient for adsorption isotherm experiments.

Batch Adsorption

Comparison of the batch As(V) adsorption to reagent grade $ZnCO_3$ and freshly precipitated $ZnCO_3$ minerals on calcite particles in buffered electrolyte solution and Rice groundwater shows interference from other other dissolved ions in groundwater. In buffered electrolyte solution, the As(V) adsorption to both zinc carbonate solids follows a Langmuir adsorption pattern. Adsorption is suppressed in the Rice groundwater solution, exhibiting a linear adsorption isotherm as seen in Figure 13.

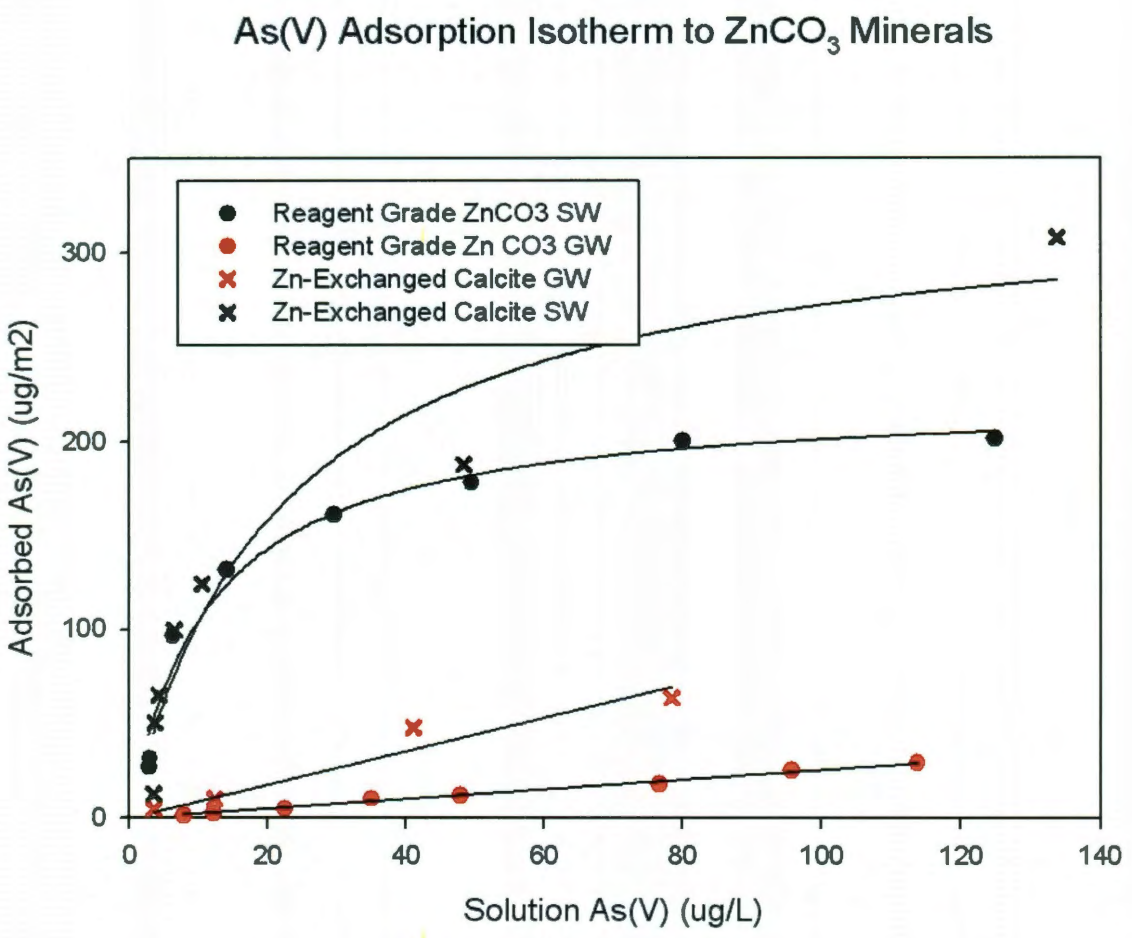

Figure 13: Batch adsorption isotherm of buffered electrolye solution (SW) and Rice groundwater (GW) with reagent grade $ZnCO_3$ and freshly precipitated $ZnCO_3$ on calcite particles

Fitted model parameters can be compared in Table 7. Adsorption to the freshly precipitated $ZnCO_3$ is greater than reagent grade solids in both buffered electrolyte and Rice groundwater solutions. This higher As(V) adsorption affinity is likely due to the higher surface energy of freshly precipitated crystals. Over time, surface ripening of crystals tends to reduce the overall surface energy through surface relaxation, in which surface atoms shift inwards, and restructuring, where dangling surface bonds are combined (Cao and Wang, 2011). Correlation of the fitted model to the data is not as good for the zinc exchanged calcite due to more heterogeneity of the surface including

possible calcite surface sites still present and different ratios of smithsonite to hydrozincite in the solid sample used for each isotherm point.

Table 7: Fitted model parameters of SW & GW batch adsorption isotherms

Solution	Solid	Isotherm Model	Q_m	K_{ads}	Units	R^2
SW	Reagent	Langmuir	223.8±11.1	0.0879±0.0160	L/μg	0.974
SW	Zn-Exchange	Langmuir	332.2±41.1	0.0454±0.0156	L/μg	0.930
GW	Reagent	Linear	--	0.2543±0.0056	L/m^2	0.991
GW	Zn-Exchange	Linear	--	0.8854±0.0843	L/m^2	0.931

Several commonly occurring groundwater constituents have shown to decrease arsenic adsorption onto other adsorptive media. Shipley et al. found that phosphate, bicarbonate, and silica had the greatest antagonistic effect on both arsenate and arsenite adsorption (2010). While high PO_4^{3-} concentrations ($\geq$5 μM) significantly decreased arsenic adsorption kinetics, PO_4^{3-} in typical groundwater levels (0.2-2.4 μM) had no significant impact on arsenic adsorption to nanomagnetite. Similarly, it was found that increasing concentration of bicarbonate and silica from 0-8.2 and 0-1.7 mM, respectively, showed decreasing adsorption of both arsenate and arsenite.

Arsenic BTC of Calcite Control Column

As(V) breakthrough in a plain $CaCO_3$ column provides a control media for comparison of retardation in the Zn^{2+} treated columns. The actual breakthrough curve was fitted using CXTFIT, as seen in Figure 14.

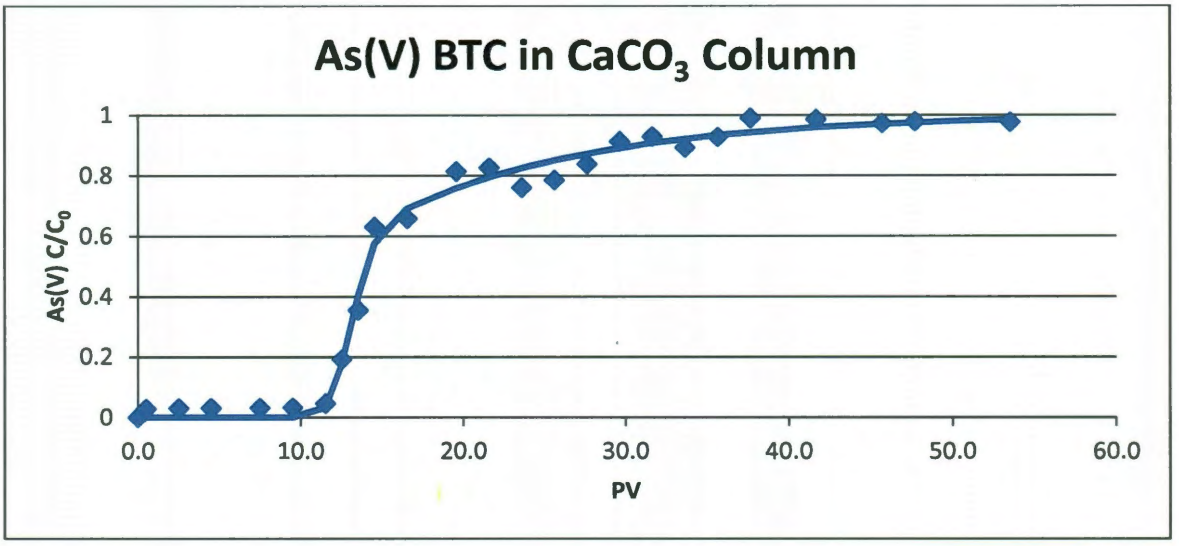

Figure 14: As(V) breakthrough in $CaCO_3$ column

The plain calcite column exhibits slight retardation of arsenic with initial breakthrough occurring around 12 PV. Fitted parameters can be seen in Table 8.

Table 8: CXTFIT model parameters of As(V) breakthrough in $CaCO_3$ media

Column	As(V) C_0 (µg/L)	R	D (cm/min)	*f*	$\mu_1(min^{-1})$	R^2
C	114	18 ± 1	8.11E-03 ± 3.26E-03	0.71±0.08	0.00±0.03	0.992

These results are in agreement with recent studies examining the sorption of arsenate onto calcite media. Alexandratos found that at pH 8.3, the maximum arsenate adsorption capacity corresponds to nearly 8% of theoretical CO_3 surface sites, indicating that arsenate adsorption only takes place at a limited number of the total available sites (2007). Based upon EFAXS analysis, the authors concluded that As(V) forms an inner-sphere complex by corner-sharing with Ca octahedral, with dominant sorption occuring on step or kink sites (Alexandratos et al., 2007).

Zn^{2+} Exchange of Iceland Spar Column

The zinc exchange treatment produced similar results for all zinc exchanged calcium carbonate columns. After 4500 pore volumes, zinc had replaced approximately 45% of the original calcium (mmol basis) with an additional 15% of zinc precipitation, as seen in Figure 15. The additional 15% zinc precipitation is likely due to further $ZnCO_3$ precipitation on calcite particles which have already exchanged surface sites with zinc.

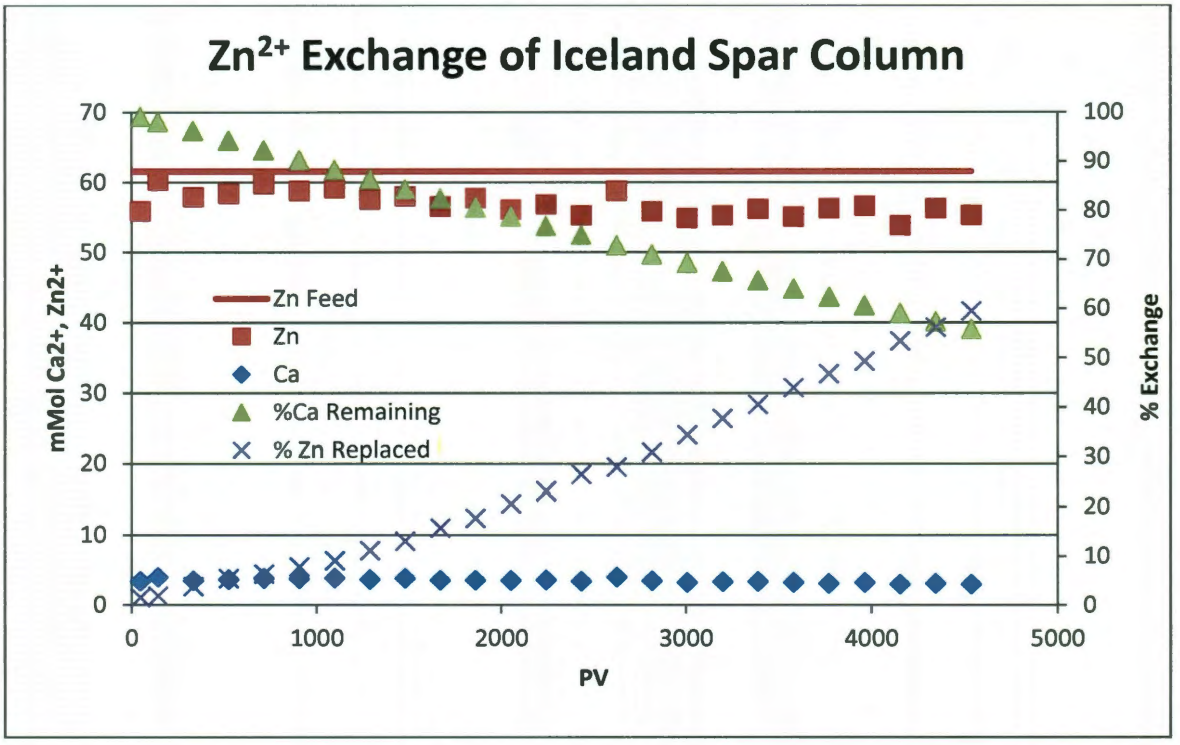

Figure 15: Effluent concentrations from typical zinc exchange of Iceland Spar column

Effluent characterization shows a slight decrease in Ca^{2+} throughout the exchange reaction, likely due to the surface precipitation of $ZnCO_3$ on calcite particles, reducing the available surface area for dissolution. Through most of the column reaction, less than 5 mM Zn^{2+} precipitated from solution. Since the primary focus of this study was arsenic removal using the exchanged media, system parameters of the Zn^{2+} exchange reaction

were not investigated. However, future work should further examine effects of pH, ionic strength, different carbonate minerals and Zn^{2+} concentration on the Zn^{2+} exchange reaction.

Characterization of exchanged particles helps to understand the treatment reaction. The one cm length column was split into four 2.5 mm thick discs to differentiate the solids along the reaction path of the column. Figure 16 confirms the presence of precipitated smithsonite and hydrozincite as well as original calcite in the final section of the column after an exchange treatment of 4500 PV.

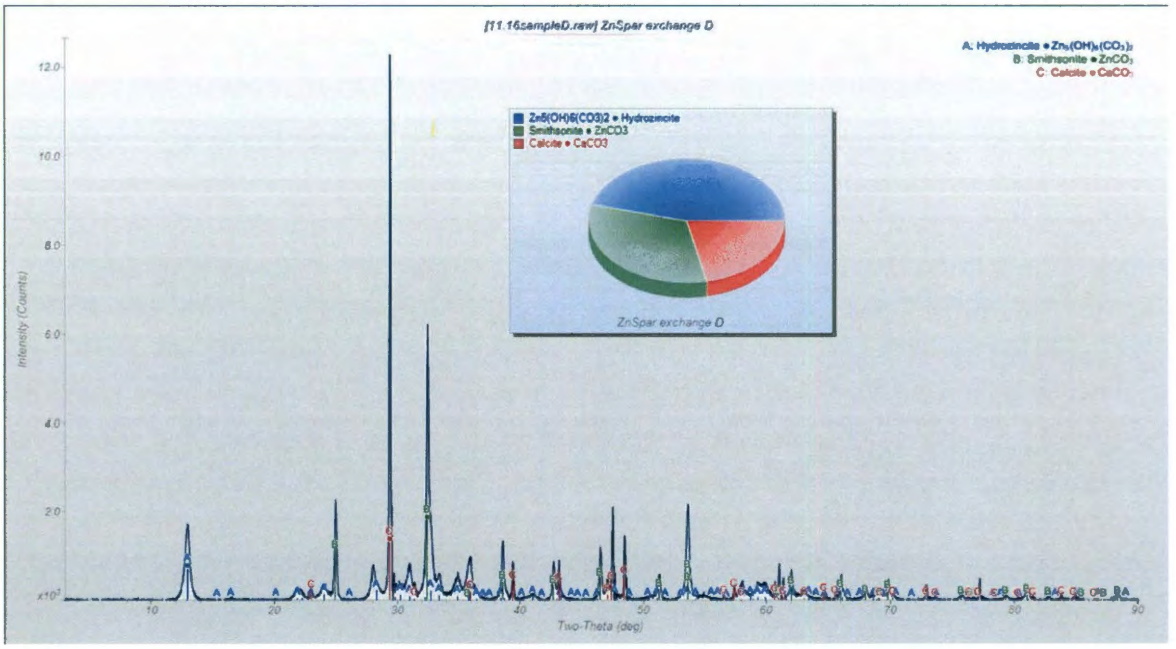

Figure 16: XRD analysis of zinc exchanged Iceland spar particles

XRD analysis of all four sections of the column confirmed the presence of the same three minerals. While XRD may be utilized for quantitative analysis of minerals present in a sample, it requires much detail in the use of internal standards and sample preparation, after which accuracy within 10-20% of the actual sample mineralogy is still considered "good" (Moore and Reynolds, 1997). Due to such high error, simple qualitative XRD

analysis was employed here for identification of phases present, and no quantitative measurement should be inferred from the relative peak intensities.

Further analysis through SEM imaging helps reveal the nature of the exchanged particle surface. Iceland spar particles from the entrance section of the column show cavitation and pitting as seen in Figure 17.

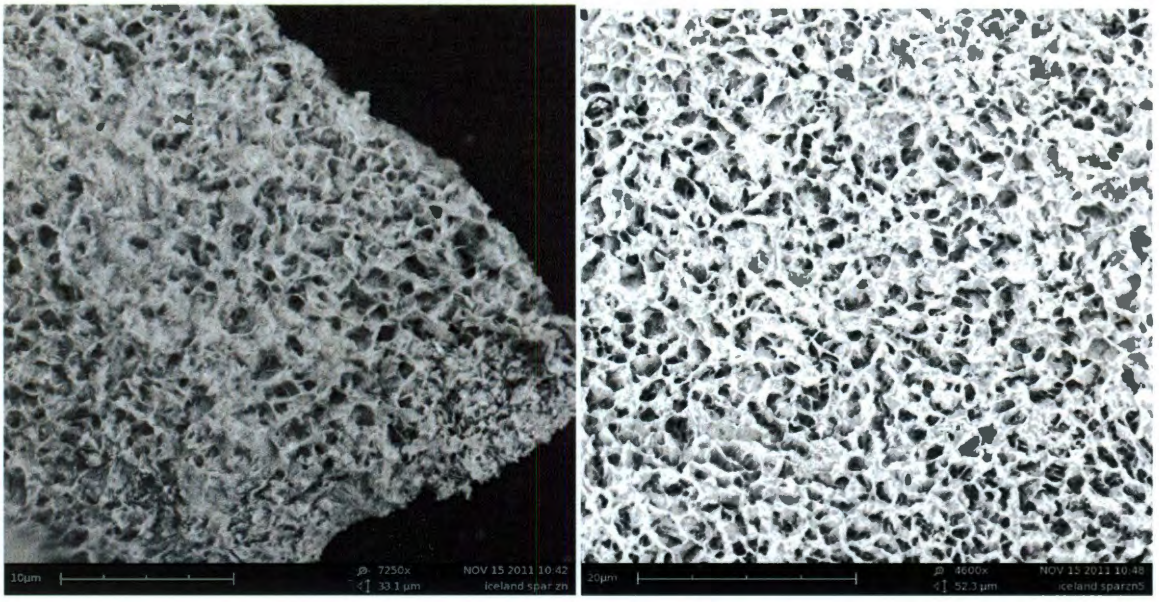

Figure 17: SEM image of column entrance section post-exchange reaction particle dissolution

The dissolution of particles at the column entrance is expected due to calcite SI < 0 of initial zinc exchange feed solution. However, this dissolution brings the solution closer to calcite equilibrium and buffers the solution slightly, such that $ZnCO_3$ exchange and precipitation is more favorable. The precipitation of smithsonite and hydrozincite from the exit section of the column can be seen in Figure 18.

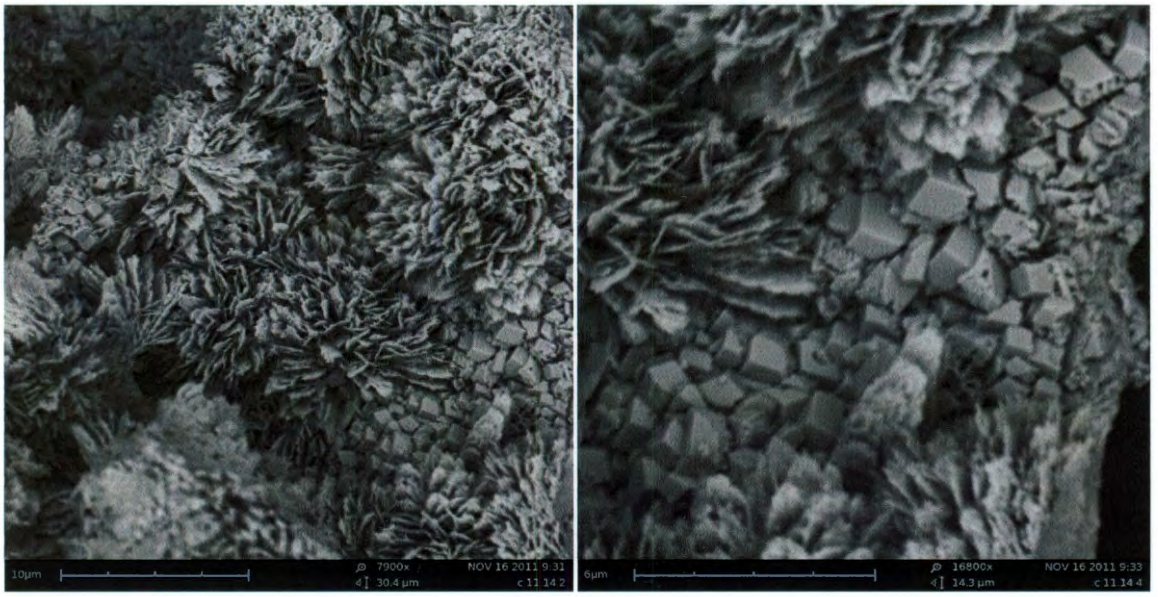

Figure 18: SEM image of precipitate on column exit section particles post-exchange

The appearance of platy, rosette style precipitates strongly resembles that of natural hydrozincite minerals while the rhombohedral aggregates appear similar to those reported as smithonsite in the literature (Boni et al., 2003).

In order to compare As(V) breakthrough in synthetic and real groundwater, the same column design was selected for exchange reaction and subsequent arsenic breakthrough. Both columns were treated with similar zinc exchange solution, resulting in near identical properties, as seen in Table 9.

Table 9: Column properties post-Zn^{2+} exchange

Column	Solution	Length (cm)	ID (cm)	Mass $CaCO_3$ (g)	PV of Zn^{2+} Treatment	Ca^{2+} Remaining (%)	Total Zn^{2+} precipitated (millimoles)
B	SW	1.0	0.66	0.5297	4425	54.7	3.25
D	GW	1.0	0.66	0.5297	4534	55.8	3.15

Based upon effluent metal analysis, the remaining Ca^{2+} and precipitated Zn^{2+} was calculated for each column. Columns B and D exhibit only 2.0% and 3.1% difference in

remaining Ca^{2+} and precipitated Zn^{2+}; therefore, the resulting arsenic breakthroughs can be compared due to similar solid fractions of each column.

Synthetic Water As(V) Breakthrough

Arsenic in the buffered electrolyte solution was retarded through the zinc-exchanged calcite media with initial breakthrough ($C/C_0 = 0.05$) occurring around 4500 PV. Nearly 6000 PV were treated before As(V) concentration exceeded the EPA MCL of 10 μg/L, as can be seen in Figure 19.

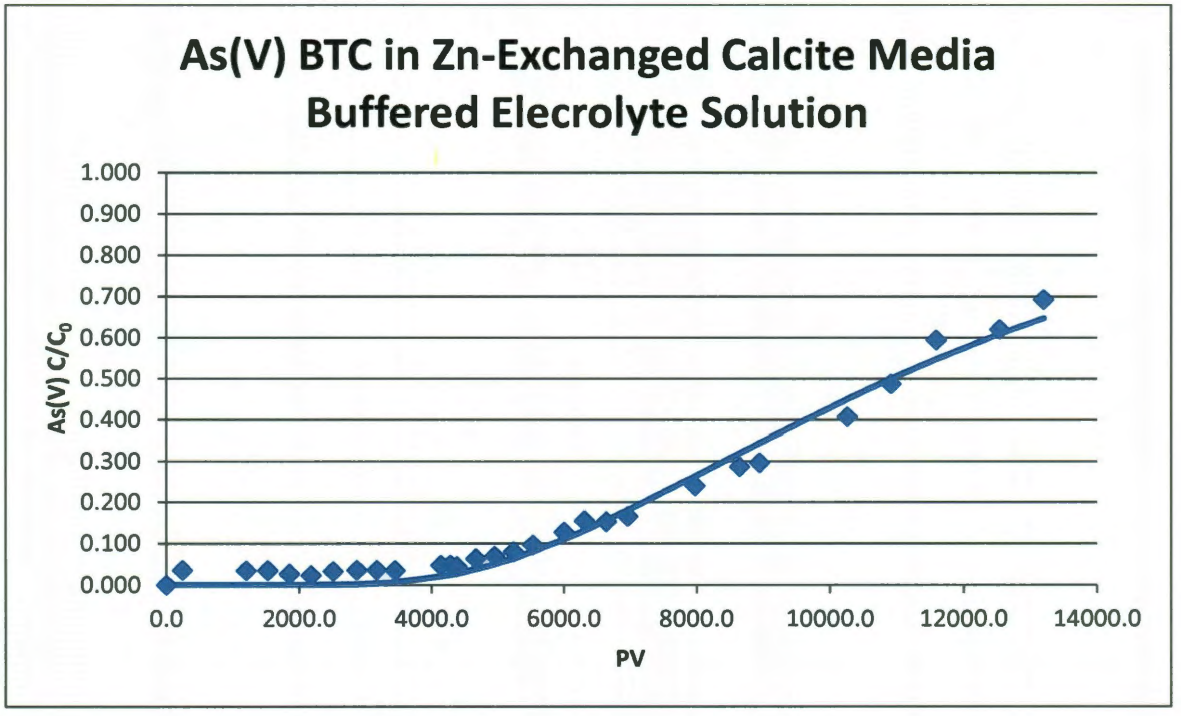

Figure 19: As(V) breakthrough of buffered electrolyte solution

The breakthrough curve is characteristic of high dispersion due to the gradual arsenic increase past initial breakthrough. As explained by Seader, a vertical "stoichiometric front" typically ascribed to ideal transport is replaced here by an S-shaped breakthrough due to a moving mass transfer zone (2011). Fitted breakthrough parameters from

CXTFIT can be seen in Table 10: CXTFIT model parameters of As(V) breakthrough in a buffered electrolyte solution in Zn-exchanged calcite mediaTable 10.

Table 10: CXTFIT model parameters of As(V) breakthrough in a buffered electrolyte solution in Zn-exchanged calcite media

Column	As(V) C_0 (µg/L)	R	D (cm/min)	R^2
B	105	12351 ± 275	3.03E-02 ± 3.06E-03	0.979

Since breakthrough has not yet reached 100% or an equilibrium plateau value, any attempt for CXTFIT to estimate a 1st order decay coefficient (µ) only adds additional deviation to the other parameters. Therefore, for all arsenic breakthrough curves in zinc-exchanged calcite media, decay on the solid phase was neglected ($\mu_s = 0$) as well as kinetic adsorption sites (f=0.999999). These assumptions produced good correlation of the fitted parameters with the data as well as reasonable standard deviations. Upon the completion of these column breakthrough experiments, the data will be refitted to determine if more accurate parameters can be modeled using the actual equilibrium breakthrough value.

Effluent Ca^{2+} and Zn^{2+} were also monitored throughout the breakthrough to gain a better understanding of the solution chemistry interaction with the solid phase. As seen in Figure 20, effluent calcium and zinc maintained concentrations of about 35 and 0.5 mg/L throughout the majority of the column study.

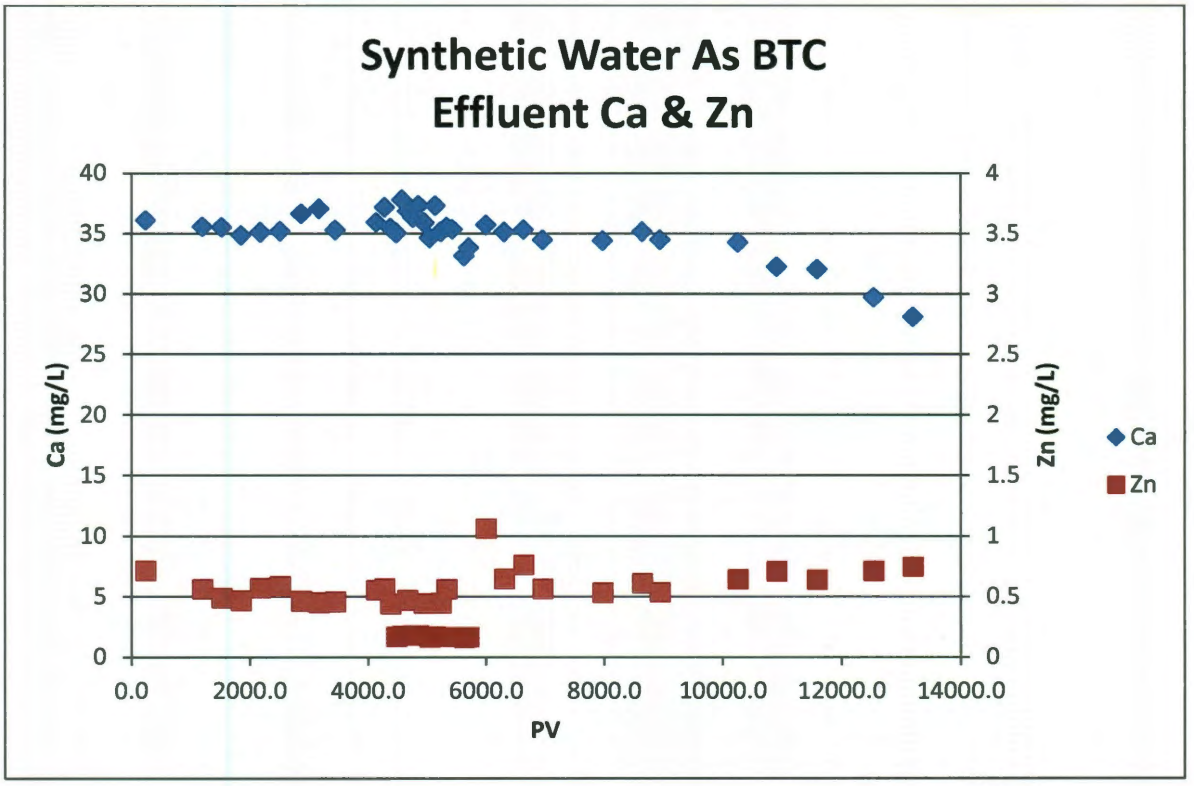

Figure 20: Effluent Ca2+ and Zn2+ of buffered electrolyte solution As(V) breakthrough

The effluent zinc concentration was well below the EPA secondary standard of 5 mg/L through over 13,000 PV. While the solution was buffered with 5 mM TRIS at an initial pH of 8.0, effluent pH was constant at 8.25 ± 0.05. The pH rise is attributed to dissolution of remaining $CaCO_3$ and zinc-carbonate solids in the column.

The effluent water quality was modeled using the aquatic chemistry equilibrium speciation model Visual MINTEQ 3.0 (Gustafsson, 2011). Since effluent alkalinity is unknown, three separate models were run with the same ionic strength (5 mM NaCl) and pH (8.25) of the solution; however, each run specified a different combination of the possible minerals precipitated in the column. The three runs included 1) calcite and hydrozincite, 2) calcite and smithonsite, and 3) calcite and $ZnCO_3(s)$. The mean $[CO_3^{2-}]$ $= 8.126*10^{-4} \pm 1.66*10^{-6}$ M; therefore, this concentration was used for total dissolved

carbonate concentration due to the small standard deviation. Using this CO_3^{2-} concentration, the modeled effluent solution produced a calcite SI = 0.03, hydrozincite SI = 2.86, smithsonite SI = 0.18, and $ZnCO_3(s)$ SI = 0.08. While these results verify the solution at equilibrium with calcite and $ZnCO_3(s)$, they convey a supersaturation with respect to hydrozincite and smithsonite. This is in disagreement with XRD analysis seen in Figure 16 which verified the presence of both hydrozincite and smithsonite. However, modeled results of groundwaters often result in supersaturation of one or more carbonate minerals (Langmuir, 1997). Possible reasoning for modeled supersaturation of groundwater compositions may be due to

1. Inaccurate or inconsistent thermodynamic data
2. Solid solution mineral phases or submicron particle sizes, with intrinsically higher solubility over well-crystallized phases normally studied
3. Difference in solution model used to define K_{sp} and natural water supersaturation calculation
4. Mineral nucleation inhibition by adsorbed substances
5. Slow nucleation and/or precipitation kinetics resulting

Therefore, this occurrence is not uncommon.

Rice Groundwater As(V) Breakthrough

Similar to arsenic breakthrough in synthetic water solution, As(V) was retarded in actual Rice groundwater through the Zn-exchanged calcite media with initial

breakthrough ($C/C_0 = 0.05$) occurring around 5500 PV. The EPA MCL of 10 µg/L arsenic was exceeded after 6500 PV, as seen in Figure 21.

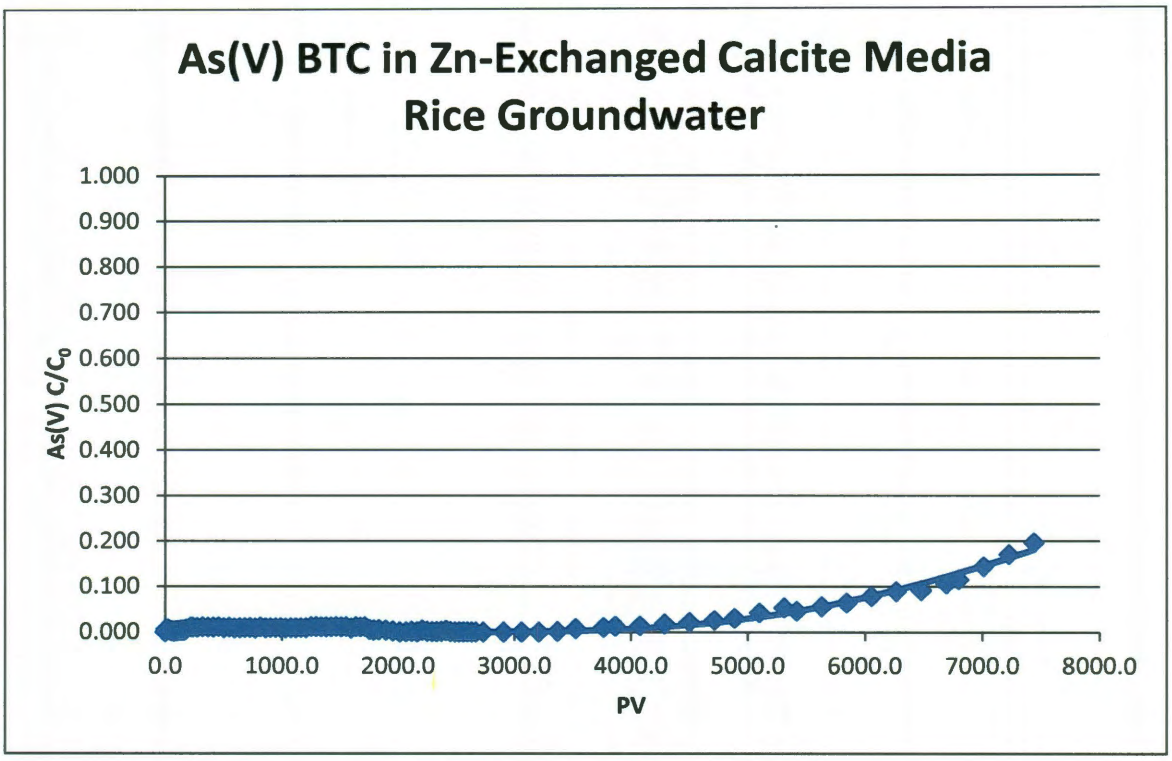

Figure 21: As(V) breakthrough of actual Rice groundwater in Zn-exchanged calcite media

This result of extended arsenic removal in actual Rice groundwater appears contradictory to the batch adsorption results, in which As(V) adsorption to $ZnCO_3$ was significantly suppressed in actual groundwater relative to the buffered electrolyte solution. Fitted model paramters from CXTFIT can be seen in Table 11.

Table 11: Model paramters of groundwater As(V) BTC using CXTFIT

Column	As(V) C_0 (µg/L)	R	D (cm/min)	R^2
D	114	12012 ± 402	2.20E-02 ± 2.26E-03	0.971

The much smaller K_d value determined from batch adsorption should decrease the R factor according to Equation 10. Further examination of the effluent constituents is necessary for elucidation of the arsenic removal mechanism.

The column effluent was monitored for Ca^{2+} and Zn^{2+} to correlate the solution chemistry to solid phases in the column. As seen in Figure 22, the Ca^{2+} stays relatively constant at 11 mg/L after an initial spike in concentration, while the Zn^{2+} steadily declines to around 0.03 mg/L.

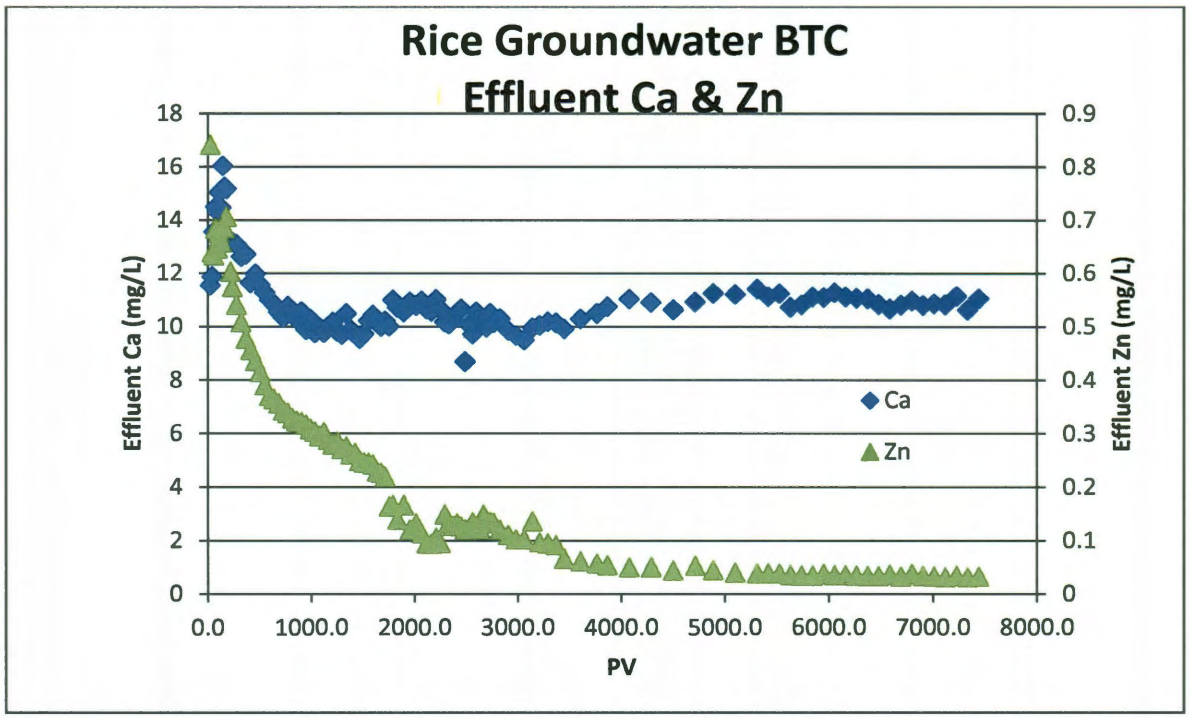

Figure 22: Effluent Ca & Zn in As(V) breakthrough in Rice groundwater solution

Effluent Ca^{2+} remains fairly constant at the initial feed concentration of 11 mg/L after an initial spike, which may be due to perturbations in the column. When the groundwater solution is modeled in Visual MINTEQ at pH 8.75 set at equilibrium with hydrozincite, the equilibrium $[Zn^{2+}] = 0.054$ mg/L. This value is very similar to the final observed zinc concentration (0.03 mg/L), confirming the presence of equilibrium with hydrozincite.

The continual decrease in Zn^{2+} concentration to this level may likely be due to aging of more soluble Zn-carbonate solids into the hydrozincite mineral.

The modeled groundwater feed solution was calculated to be slightly supersaturated with respect to several minerals including siderite ($FeCO_3$ SI = 0.124), sepiolite ($Mg_4Si_6O_{15}(OH)_26H_2O$ SI = 0.287), disordered dolomite ($CaMg(CO_3)_2$ SI = 0.516), calcite ($CaCO_3$ SI = 0.635), chrysotile ($Mg_3(Si_2O_5)(OH)_4$ SI = 0.866), and highly supersaturated with respect to greenalite ($Fe_2Si_2O_5OH_4$ SI = 5.394). The slight oversaturation of these minerals is not expected to provide a strong driving force for precipitation; however, the high saturation index of greenalite may induce nucleation depending on kinetics. The breakthrough of major groundwater constituents can be seen in Figure 23 relative to feed concentration (C/C_0) .

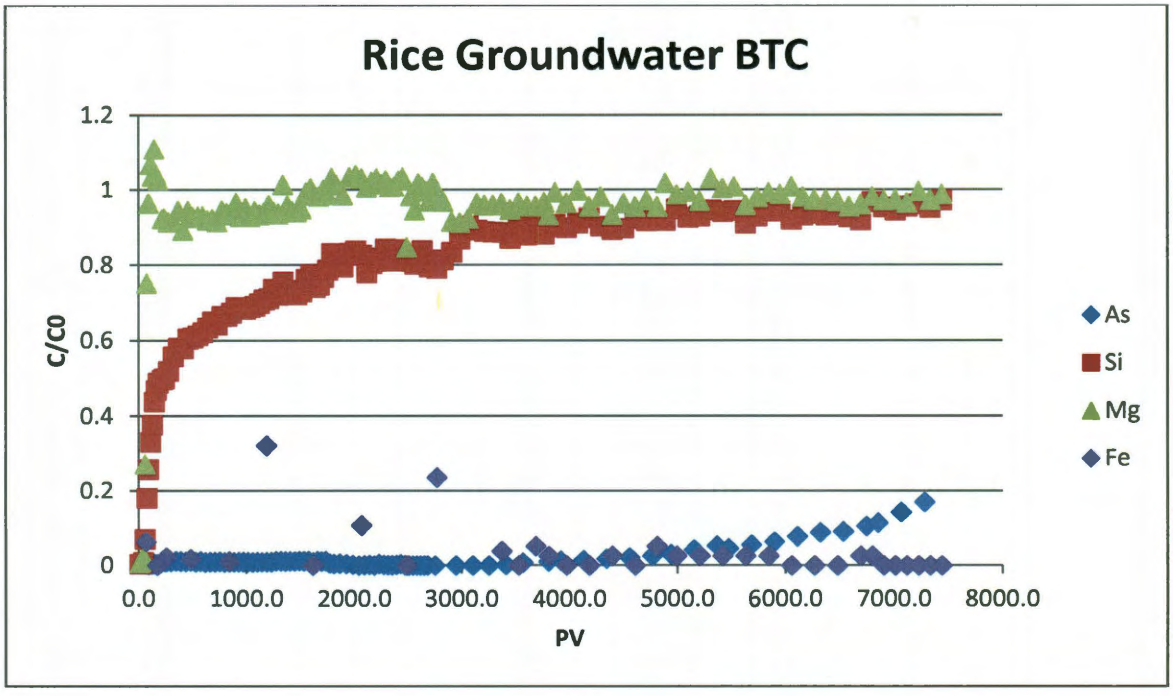

Figure 23: As, Si, Mg, & Fe breakthrough in Rice groundwater solution

While Mg^{2+} reaches 100% breakthrough in about 100 PV, silica and iron both show differing retardation profiles. Silica breakthrough reaches 50% around 200 PV but

exhibits an extended shoulder profile which continues up to 95% breakthrough at 7500 PV. Iron, however, is almost completely removed from the system throughout the duration of the column experiment.

There are several possible explanations for the iron removal. Any Fe(II) may adsorb onto the solid surface as an ion-exchange process, displacing other adsorbed ions, or exchange with the $CaCO_3$ or $ZnCO_3$ solids into an $FeCO_3$ solid. The iron removal may also be due to greenalite precipitation in the column, evidenced by high SI value. This would provide additional surface sites for adsorption of a soluble zinc-arsenate complex, as described by Grafe (2004) and Yang (2011), thereby supporting As(V) adsorption beyond the expected R value based upon batch adsorption studies. However, since the groundwater solution is aerated prior to experiments, it is likely that most iron in solution has oxidized to Fe(III). When the groundwater solution is modeled with Fe(III), the solution is supersaturated with respect to several iron oxides including ferrihydrite (SI = 4.14), goethite (α-FeOOH SI = 6.84), hematite (α-Fe_2O_3 SI = 16.09), lepidocrocite (γ-FeOOH SI = 5.96), maghemite (γ-Fe_2O_3 SI = 8.28), and magnesioferrite ($MgFe_2O_4$ SI = 11.23). The precipitation of these iron oxides would also provide surface hydroxyl groups (≡FeOH) for additional adsorption capacity of the zinc-arsenate complex described above.

Another possible mechanism for extended arsenic removal in the real groundwater solution could be due to incorporation into a separate precipitating phase. For example, natural specimens of the zinc-silicate mineral hemimorphite ($Zn_4(Si_2O_7)(OH)_2H_2O$) have been shown to contain significant amounts (up to 300 ppm) of lattice bound arsenate (Mao et al., 2010). The authors concluded that hemimorphite

was an ideal candidate for arsenate incorporation due to zeolite-like lattice structure and stereochemical similarities between AsO_4^{3-} and SiO_4^{4-}. It is possible that some arsenic removal in the groundwater solution column may be due to arsenate substitution for SiO_4^{4-} groups in hemimorphite or other precipitating silicate minerals. The lack of 100% silica breakthrough in the column also provides support that a silicate precipitation is possible. Precipitation would also provide additional surface area for sorption of a zinc-arsenate complex. Using limited thermodynamic data available for willemite (Brugger et al., 2003; Robie et al., 1978) the groundwater effluent solution is estimated to be highly supersaturated with an SI of 4.85. Unfortunately, thermodynamic predictions of hemimorphite stability in this solution cannot be made due to lack of solubility data (Brugger et al., 2003; McPhail et al., 2006). While the high willemite saturation index does not necessitate precipitation due to reaction kinetics, it does indicate a strong thermodynamic driving force for this mechanism.

The mechanism of As(V) removal in the groundwater solution through the Zn-exchanged calcite media should be better understood once 100% arsenic breakthrough is achieved and the column solids can be analyzed. XRD analysis of solids from multiple locations along the length of the column should elucidate what, if any, other mineral phases are precipitating inside the column.

5. Conclusion

Adsorption of arsenic onto zinc carbonate solids and potential for *in situ* zinc-exchange with calcite minerals was studied in both simple electrolyte and actual groundwater solutions. Batch adsorption experiments show $ZnCO_3$ minerals have a high affinity for As(V), with freshly precipitated crystals having slightly larger partitioning coefficient than reagent grade solids. Adsorption was suppressed in actual groundwater solutions due to competitive adsorption from other groundwater constituents such as silica and bicarbonate. Injection of concentrated zinc solutions through calcite columns showed around 50% exchange of mineral form in 4500 PV and precipitation of both smithsonite ($ZnCO_3$) and hydrozincite ($Zn_5(CO_3)_2(OH)_6$). Transport of 100 μg/L As(V) was significantly impeded through the zinc-treated calcite with R factor greater than 12,000 for both synthetic and actual groundwater solutions. While arsenic removal from synthetic solutions is due to the high affinity of As(V) for zinc carbonate solids, other possible mechanisms may explain the unexpectedly high removal efficiency in groundwater solutions containing adsorption-interfering ions. Plausible explanations for As(V) removal may be due to incorporation into zinc-silicate minerals such as willemite (Zn_2SiO_4) or hemimorphite ($Zn_4Si_2O_7(OH)_2H_2O$), or preferential adsorption over other groundwater constituents due to the high sorption affinity of an aqueous zinc-arsenate complex seldom described in the literature.

6. Future Research

The high adsorption affinity of arsenic for zinc carbonate minerals provides great promise for an *in situ* treatment of arsenic contaminated groundwaters and leaves numerous questions for future research. Additional investigation is needed regarding the impact of solution conditions such as pH and Zn^{2+} concentration on the exchange reaction with carbonate minerals and precipitation. Also, the interaction of elevated zinc levels with other common soil constituents such as silicates, clays, and iron oxides should be studied to understand the role they may take in altering groundwater zinc and arsenic concentration. Due to the success of zinc carbonate, other less soluble minerals should be examined for *in situ* exchange reaction and groundwater contaminant removal.

Further studies should also examine the aqueous zinc-arsenate complex due to the high sorption affinity to iron oxide surface sites described in the literature and zinc carbonate solids seen here. Future research should investigate the use of zinc to enhance arsenic removal in conventional treatment technologies. Additional research is needed to study the adsorption of As(III) onto zinc carbonate minerals and determine if the zinc-exchange reaction is applicable to both forms of inorganic arsenic. Solution parameters such as pH, salinity, and common interfering ions in groundwater such as silica, bicarbonate, and phosphate should be studied to determine applicable solution conditions where zinc-exchange is successful for arsenic removal.

7. References

Alexandratos, V.G., Elzinga, E.J., Reeder, R.J., 2007. Arsenate uptake by calcite: Macroscopic and spectroscopic characterization of adsorption and incorporation mechanisms. Geochimica Et Cosmochimica Acta, 71(17): 4172-4187.

Arai, Y., Sparks, D.L., Davis, J.A., 2005. Arsenate adsorption mechanisms at the allophane - water interface. Environmental Science & Technology, 39(8): 2537-2544.

Ayotte, J.D., Montgomery, D.L., Flanagan, S.M., Robinson, K.W., 2003. Arsenic in groundwater in eastern New England: Occurrence, controls, and human health implications. Environmental Science & Technology, 37(10): 2075-2083.

Boni, M., Gilg, H.A., Aversa, G., Balassone, G., 2003. The "calamine" of southwest Sardinia: Geology, mineralogy, and stable isotope geochemistry of supergene Zn mineralization. Economic Geology and the Bulletin of the Society of Economic Geologists, 98(4): 731-748.

Brookins, D.G., 1988. Eh-PH diagrams for geochemistry. Springer-Verlag, Berlin ; New York, viii, 176 p. pp.

Brugger, J., McPhail, D.C., Wallace, M., Waters, J., 2003. Formation of willemite in hydrothermal environments. Economic Geology and the Bulletin of the Society of Economic Geologists, 98(4): 819-835.

Bureau, U.C., 2008. American Housing Survey for the United States: 2007. In: Development, U.D.o.H.a.U. (Editor). Current Housing Reports, H150/07. US Government Printing Office, Washington D.C.

Cameron, D.R., Klute, A., 1977. Convective-Dispersive Solute Transport with a Combined Equilibrium and Kinetic Adsorption Model. Water Resources Research, 13(1): 183-188.

Cao, G., Wang, Y., 2011. Nanostructures & nanomaterials : synthesis, properties, and applications. World scientific series in nanoscience and nanotechnology. World Scientific, New Jersey, xiii, 581 p. pp.

Clifford, D., 1999. Presentation at Arsenic Technical Work Group, Washington, D.C.

Cornell, R.M., Schwertmann, U., 2003. The iron oxides : structure, properties, reactions, occurrences, and uses. Wiley-VCH, Weinheim, xxxix, 664 p. pp.

Cullen, W.R.a.R., Kenneth J., 1989. Arsenic speciation in the environment. Chemical Reviews, 89(4): 713-764.

Dixon, J.B., Weed, S.B., Dinauer, R.C., 1989. Minerals in soil environments. Soil Science Society of America book series. Soil Science Society of America, Madison, Wis., USA, xxvii, 1244 p. pp.

DOD, 1998. Evaluation of DOD Waste Site Groundwater Pump-and-Treat Operations. In: Defense, D.o. (Editor). Inspector General Evaluation Report.

DPHE, B.a., 2001. Arsenic contamination of groundwater in Bangladesh, British Geological Survey, Keyworth, UK.

Dregne, H.E., 1976. Soils of arid regions. Developments in soil science. Elsevier Scientific Pub. Co., Amsterdam ; New York, xii, 237 p. pp.

Dzombak, D.A., Morel, F.o.M.M., 1990. Surface complexation modeling : hydrous ferric oxide. Wiley, New York, xvii, 393 p. pp.

EPA, 1989. Evaluation of Groundwater Extraction Remedies. In: Responses, O.o.E.a.R. (Editor), Washington, DC.
EPA, 2001. Technical Fact Sheet: Final Rule for Arsenic in Drinking Water, Washington, D.C.
EPA, 2003. Arsenic Treatment Technology Evaluation Handbook for Small Systems. In: Water, O.o. (Editor), Washington, D.C., pp. 1-151.
EPA, 2005. Toxicological Review of Zinc and Compounds. EPA, Washington D.C., pp. 83.
EPA, 2009. National Primary Drinking Water Regulations. In: EPA (Editor), Washington DC.
Fischer, P.W.F., Giroux, A., Labbe, M.R., 1984. EFFECT OF ZINC SUPPLEMENTATION ON COPPER STATUS IN ADULT MAN. American Journal of Clinical Nutrition, 40(4): 743-746.
Ford, D., Williams, P.W., 2007. Karst hydrogeology and geomorphology. John Wiley & Sons, Chichester, England ; a Hoboken, NJ, ix, 562 p. pp.
Gibert, O., de Pablo, J., Cortina, J.L., Ayora, C., 2010. In situ removal of arsenic from groundwater by using permeable reactive barriers of organic matter/limestone/zero-valent iron mixtures. Environmental Geochemistry and Health, 32(4): 373-378.
Grafe, M., Nachtegaal, M., Sparks, D.L., 2004. Formation of metal-arsenate precipitates at the goethite-water interface. Environmental Science & Technology, 38(24): 6561-6570.
Gustafsson, J.P., 2011. Visual MINTEQ 3.0, Stockholm, Sweden.
Henke, K.R., 2009. Arsenic : environmental chemistry, health threats, and waste treatment. Wiley, Hoboken, NJ.
IARC, 2004. Summaries & evaluations: Arsenic in drinking water, IARC, Lyon.
Joint FAO/WHO Expert Committee on Food Additives., 1982. Evaluation of certain food additives and contaminants : twenty-sixth report of the Joint FAO/WHO Expert Committee on Food Additives. Technical report series / World Health Organization. World Health Organization ;
WHO Publications Centre USA distributor, Geneva
Albany, N.Y., 51 p. pp.
Keller, A.A., Sirivithayapakorn, S., Chrysikopoulos, C.V., 2004. Early breakthrough of colloids and bacteriophage MS2 in a water-saturated sand column. Water Resources Research, 40(8).
Kinniburgh, D.G., Smedley, P.L., 2001. Arsenic contamination of groundwater in Bangladesh. BGS technical report. British Geological Survey, Keyworth.
Koziol, A.M., Newton, R.C., 1995. Experimental determination of the reactions magnesite plus quartz equals enstatite plus CO2 and magnesite equals periclase plus CO2, and enthalpies of formation of enstatite and magnesite. American Mineralogist, 80(11-12): 1252-1260.
Langmuir, D., 1997. Aqueous environmental geochemistry. Prentice Hall, Upper Saddle River, N.J., viii, 600 p. pp.
Malle, K.G., 1992. ZINC IN THE ENVIRONMENT. Zeitschrift Fur Wasser- Und Abwasser-Forschung-Journal for Water and Wastewater Research-Acta Hydrochimica Et Hydrobiologica(4): 196-204.

McPhail, D.C., Summerhayes, E., Jayaratne, V., Christy, A., 2006. Hemimorphite solubility and stability of low-T zinc minerals. Geochimica Et Cosmochimica Acta, 70(18): A414-A414.

Milne, D.B., Davis, C.D., Nielsen, F.H., 2001. Low dietary zinc alters indices of copper function and status in postmenopausal women. Nutrition, 17(9): 701-708.

Moore, D.M., Reynolds, R.C., 1997. X-ray diffraction and the identification and analysis of clay minerals. Oxford University Press, Oxford ; New York, xviii, 378 p. pp.

Nath, B. et al., 2009. Mobility of arsenic in the sub-surface environment: An integrated hydrogeochemical study and sorption model of the sandy aquifer materials. Journal of Hydrology, 364(3-4): 236-248.

Nordstrom, D.K. et al., 1990. Revised Chemical-Equilibrium Data for Major Water-Mineral Reactions and Their Limitations. Acs Symposium Series, 416: 398-413.

NRC, 1994. Alternatives for ground water cleanup. National Academy Press, Washington, D.C., xvi, 315 p. pp.

Parker, J.C.M.T.v.G., 1984. Determining Transport Parameters from Laboratory and Field Tracer Experiments, Virginia Agricultural Experiment Station Bulletin, Blacksburg, VA.

Pote, J. et al., 2003. Fate and transport of antibiotic resistance genes in saturated soil columns. European Journal of Soil Biology, 39(2): 65-71.

Preis, W., Gamsjager, H., 2001. Thermodynamic investigation of phase equilibria in metal carbonate-water-carbon dioxide systems. Monatshefte Fur Chemie, 132(11): 1327-1346.

Quantachrome, 2004. Autosorb AS-3B & AS-6B Multistation Gas Sorption System Users Manual. Quantachrome Instruments, Boynton Beach, FL.

Raven, K.P., Jain, A., Loeppert, R.H., 1998. Arsenite and arsenate adsorption on ferrihydrite: Kinetics, equilibrium, and adsorption envelopes. Environmental Science & Technology, 32(3): 344-349.

Ravenscroft, P., 2007. Predicting the Global Extent of Arsenic Pollution of Groundwater and Its Potential Impact on Human Health, UNICEF, Cambridge.

Robie, R.A., Hemingway, B.S., Fisher, J.R., 1978. Thermodynamic properties of minerals and related substances at 298.15K and 1 bar (10^5 pascals) pressure and at higher temperatures. Geological Survey bulletin 1452. U.S. Govt. Print. Off., Washington, iii, 456 p. pp.

Romero, F.M., Armienta, M.A., Carrillo-Chavez, A., 2004. Arsenic sorption by carbonate-rich aquifer material, a control on arsenic mobility at Zimapan, Mexico. Archives of Environmental Contamination and Toxicology, 47(1): 1-13.

RTDF, E., 1998. Permeable Reactive Barrier Technologies for Contaminant Remediation. In: RTDF, E. (Editor), Washington DC.

Ryker, S.J., 2001. Mapping arsenic in groundwater: A real need, but a hard problem - Why was the map created? Geotimes, 46(11): 34-36.

Ryu, J.H., Gao, S.D., Dahlgren, R.A., Zierenberg, R.A., 2002. Arsenic distribution, speciation and solubility in shallow groundwater of Owens Dry Lake, California. Geochimica Et Cosmochimica Acta, 66(17): 2981-2994.

Sandstead, H.H., 1994. UNDERSTANDING ZINC - RECENT OBSERVATIONS AND INTERPRETATIONS. Journal of Laboratory and Clinical Medicine, 124(3): 322-327.

Seader, J.D., Henley, E.J., Roper, D.K., 2011. Separation process principles : chemical and biochemical operations. Wiley, Hoboken, NJ, xxvi, 821 p. pp.

Shipley, H.J., Yean, S., Kan, A.T., Tomson, M.B., 2010. A sorption kinetics model for arsenic adsorption to magnetite nanoparticles. Environmental Science and Pollution Research, 17(5): 1053-1062.

Smedley, P.L., Kinniburgh, D.G., 2002. A review of the source, behaviour and distribution of arsenic in natural waters. Applied Geochemistry, 17(5): 517-568.

Smedley, P.L., Nicolli, H.B., Macdonald, D.M.J., Barros, A.J., Tullio, J.O., 2002. Hydrogeochemistry of arsenic and other inorganic constituents in groundwaters from La Pampa, Argentina. Applied Geochemistry, 17(3): 259-284.

Smith, R.M., Martell, A.E., and Motekaitis, R.J., 2001. NIST critically selected stability constants of metal complexes database. NIST standard reference database, version 6.0. In: NIST (Editor), Gaithersburg, MD.

Stewart, R., 2009. Environmental Science in the 21st Century. In: Stewart, R. (Editor), College Station, TX.

Stumm, W., Morgan, J.J., 1996. Aquatic chemistry : chemical equilibria and rates in natural waters. Environmental science and technology. Wiley, New York, xvi, 1022 p. pp.

Tanaka, T., 1988. Distribution of arsenic in the natural environment with emphasis on rocks and soils. Applied Organometallic Chemistry, 2(4): 283-295.

Thiruverikatachari, R., Vigneswaran, S., Naidu, R., 2008. Permeable reactive barrier for groundwater remediation. Journal of Industrial and Engineering Chemistry, 14(2): 145-156.

Toride, N., Leij, F.J., and M. Th. van Genuchten, 1995. The CXTFIT Code for Estimating Transport Parameters from Laboratory or Field Tracer Experiments Version 2.0, US Salinity Laboratory, USDA, Riverside, CA.

van Halem, D., Bakker, S. A., Amy, G. L., & van Dijk, J. C., 2009. Arsenic in drinking water: a worldwide water quality concern for water supply companies. Drinking Water Engineering & Science, 2: 29-34.

Wagman, D.D. et al., 1982. The Nbs Tables of Chemical Thermodynamic Properties - Selected Values for Inorganic and C-1 and C-2 Organic-Substances in Si Units. Journal of Physical and Chemical Reference Data, 11: 1-&.

Walsh, C.T., Sandstead, H.H., Prasad, A.S., Newberne, P.M., Fraker, P.J., 1994. ZINC - HEALTH-EFFECTS AND RESEARCH PRIORITIES FOR THE 1990S. Environmental Health Perspectives, 102: 5-46.

Wang, S.L., Zhao, X.Y., 2009. On the potential of biological treatment for arsenic contaminated soils and groundwater. Journal of Environmental Management, 90(8): 2367-2376.

WHO, 2001. United Nations Synthesis Report on Arsenic in Drinking Water, WHO, Geneva.

WHO, 2003. Zinc in Drinking-water: Background document for development of WHO Guidelines for Drinking-water Quality, World Health Organization, Geneva.

WHO, 2010. Exposure to Arsenic: A Major Public Health Concern, WHO, Geneva.

WHO, 2011. Guidelines for drinking-water quality. World Health Organization, Geneva, xxiii, 541 p. pp.

Yadrick, M.K., Kenney, M.A., Winterfeldt, E.A., 1989. IRON, COPPER, AND ZINC STATUS - RESPONSE TO SUPPLEMENTATION WITH ZINC OR ZINC AND IRON IN ADULT FEMALES. American Journal of Clinical Nutrition, 49(1): 145-150.

Yang, W.C., Kan, A.T., Chen, W., Tomson, M.B., 2010. pH-dependent effect of zinc on arsenic adsorption to magnetite nanoparticles. Water Research, 44(19): 5693-5701.

Zeng, H., Arashiro, M., Giammar, D.E., 2008. Effects of water chemistry and flow rate on arsenate removal by adsorption to an iron oxide-based sorbent. Water Research, 42(18): 4629-4636.